Article type: **Research Advances**

Axon-dependent expression of YAP/TAZ mediates Schwann cell remyelination but not proliferation after nerve injury

Matthew Grove, Hyunkyoung Lee, and Young-Jin Son*

Shriners Hospitals Pediatric Research Center and Center for Neural Repair and Rehabilitation, Department of Anatomy and Cell Biology, Lewis Katz School of Medicine, Temple University, Philadelphia, PA 19140

* Corresponding author: Young-Jin Son, PhD
Tel: (215) 926-9354
Email: yson@temple.edu

ABSTRACT

YAP and TAZ are transcriptional regulators that powerfully stimulate cell proliferation, which drives developmental or tumorigenic tissue growth. Previously we showed that YAP/TAZ initiate and maintain Schwann cell (SC) differentiation, thereby forming and maintaining myelin sheath around peripheral axons (Grove et al., 2017). Here we show that YAP/TAZ are required for SCs to restore peripheral myelination after nerve injury. We find that YAP/TAZ dramatically disappear from denervated, proliferating SCs of adult mice after peripheral nerve injury. They reappear in SCs as axons regenerate. YAP/TAZ ablation does not impair SC proliferation or transdifferentiation into growth promoting repair SCs. SCs lacking YAP/TAZ, however, fail to upregulate myelin-associated genes and completely fail to remyelinate regenerated axons. We also show that both YAP and TAZ are required for optimal remyelination. These findings indicate that axons regulate transcriptional activity of YAP/TAZ in adult SCs and that YAP/TAZ are essential for functional regeneration of peripheral nerve.

INTRODUCTION

YAP (Yes-associated protein) and TAZ (Transcriptional coactivator with PDZ-binding motif), are paralogous transcription coactivators, chiefly known as potent stimulators of cellular proliferation in diverse developing (von Gise et al., 2012; Zhang et al., 2012; Xin et al., 2013; Cotton et al., 2017) and neoplastic (Yu et al., 2015; Zanconato et al., 2016; Moon et al., 2018) tissues. Consistent with this role, we and others have recently shown that YAP/TAZ promote vigorous proliferation of immature Schwann cells (SC) in developing peripheral nerves (Poitelon et al., 2016; Deng et al., 2017; Grove et al., 2017), and that overexpression of YAP/TAZ promotes tumorigenic proliferation of mature SCs in adult peripheral nerves (Mindos et al., 2017; Wu et al., 2018). Unexpectedly, several groups demonstrated that YAP or YAP/TAZ promote differentiation of developing SCs by upregulating myelin-associated genes, thereby mediating developmental myelination (Fernando et al., 2016; Lopez-Anido et al., 2016; Poitelon et al., 2016; Deng et al., 2017; Grove et al., 2017). Our group additionally showed that YAP/TAZ are selectively expressed in differentiated myelin-forming SCs, and that they are required for maintenance of the myelin sheath in adult nerves (Grove et al., 2017). In many systems, YAP/TAZ shift to the cytoplasm concomitant with differentiation of developing cells, and the nuclear exclusion of YAP/TAZ is believed to be required for adult cellular homeostasis (Varelas, 2014; Wang et al., 2018). It was therefore surprising to find that YAP/TAZ are nuclear and transcriptionally active in mature SCs maintaining peripheral myelination.

Building on these findings in developing and intact adult nerves, we now report on the role of YAP/TAZ in the regenerating nerve, in which SCs both proliferate and differentiate, as in developing peripheral nerve. Following traumatic nerve injury, SCs in axotomized nerve rapidly dedifferentiate and proliferate as they convert to regeneration promoting, “repair” SCs (Jessen and Mirsky, 2016; Tricaud and Park, 2017). When repair SCs regain axon contacts, they re-differentiate to myelin-forming SCs, thereby restoring motor and sensory functions (Fex Svennigsen and Dahlin, 2013; Stassart et al., 2013). Strikingly, we found that YAP/TAZ disappear from denervated SCs but reappear as the SCs regain axon contacts. Consistent with these observations, we found that YAP/TAZ are dispensable for SC proliferation after injury but required for remyelination of regenerated axons. These findings extend the role of YAP/TAZ to

functional regeneration of injured nerves and support the notion that the primary function of YAP/TAZ in adult nerves, under physiological conditions, is to maintain and repair myelination.

RESULTS

YAP/TAZ expression in Schwann cells is axon-dependent

We first examined YAP/TAZ expression in sciatic nerves of adult mice after nerve transection (Figure 1A, B, C). We tied both ends of the transected nerve to prevent axon regeneration from proximal to distal stumps, and then determined if nerve injury or axon degeneration alters nuclear localization of YAP/TAZ in adult SCs (Figure 1A). We killed these mice 1, 3, 6, 9, 12, and 24 days post injury (dpi) and immunostained proximal and distal stumps with an antibody specific for both YAP and TAZ (Grove et al., 2017). At 1 dpi, YAP/TAZ expression in SCs of the distal stump was unchanged (data not shown). Notably, at 3 dpi when axon degeneration was robust, YAP/TAZ were almost undetectable in most SC nuclei, and at 12 dpi, YAP/TAZ remained undetectable in SCs in distal stumps (Figure 1B). We also used an antibody specific for transcriptionally inactive, phosphorylated YAP (p-YAP), which is located preferentially in cytoplasm and exhibits perinuclear and membrane accumulation (Grove et al., 2017). We found that p-YAP became almost undetectable in SCs of distal stumps by 12 dpi (Figure 1C). Therefore, both nuclear and cytoplasmic YAP/TAZ are dramatically downregulated, concomitant with axon degeneration in axotomized nerve, and they remain undetectable in denervated SCs.

To test further whether expression of YAP/TAZ in SCs is axon-dependent, we next crushed sciatic nerves and permitted axons to regenerate into the distal stump (Figure 1D). Similar to transected nerves, at 3 dpi, when axons have robustly degenerated but not yet regenerated into the distal stump, YAP/TAZ were not detectable in most SCs (Figure 1E). Remarkably, at 6 dpi, when axons regenerated into the distal stump, they reappeared in the nuclei of many SCs (Figure 1E). By 12 dpi, as axon regeneration progressed, many more SCs exhibited strong nuclear YAP/TAZ. We also detected p-YAP in SCs at 12 dpi, suggesting that cytoplasmic expression of YAP/TAZ also recovers as denervated SCs make axon contacts (data not shown).

Western blotting also revealed marked reduction of YAP and TAZ levels at 3 dpi, followed by rapid upregulation of TAZ levels in crushed nerves (Figure 1F, Figure 1-figure supplement 1B). Notably, YAP levels remained low in nerve lysates at 12 dpi (Figure 1F, Figure 1-figure

supplement 1A). As cells other than SCs can affect overall YAP levels (Gaudet et al., 2011; Stierli et al., 2018), we next examined expression of YAP in SCs of crushed nerves by immunohistochemistry. We first verified that an antibody specifically recognized YAP, but not TAZ (Figure 1-figure supplement 1C). This YAP antibody revealed many SCs with nuclear YAP at or after 6 dpi (Figure 1-figure supplement 1D), demonstrating that YAP is also upregulated in SCs concomitant with axon regeneration. Notably, staining intensity of nuclear YAP frequently appeared weak even at 24 dpi, indicating that SCs of regenerated nerves may express YAP at reduced levels. Collectively, as YAP/TAZ are transcriptionally active in the nucleus, dramatic loss of YAP/TAZ in denervated SCs indicates that SCs are critically dependent on axons for the transcriptional activity of YAP/TAZ.

YAT/TAZ are dispensable for Schwann cell proliferation after nerve injury

SCs rapidly dedifferentiate and convert to repair SCs after nerve injury. During this transdifferentiation process, SCs begin to proliferate ~3 dpi (Clemence et al., 1989; Jessen and Mirsky, 2016; Tricaud and Park, 2017). Our observation that YAP/TAZ disappear in SCs by 3 days after axotomy raises the interesting possibility that YAP/TAZ are not involved in injury-elicited SC proliferation. Alternatively, levels of YAP/TAZ that are too low to be detected by immunohistochemistry may be sufficient to promote transcription of the genes activating SC proliferation. To test these possibilities, we used an inducible knockout mouse (*Plp1-creERT2; $Yap^{fl/fl}$; $Taz^{fl/fl}$*, hereafter Yap/Taz iDKO) to inactivate YAP/TAZ selectively in SCs after nerve injury. We induced recombination at 6 weeks of age, transected the sciatic nerve in one leg, killed the mice 5 days later when SCs actively proliferate, and compared SC proliferation in intact and transected nerves of WT and iDKO mice (Figure 2A, n=3 mice per genotype). We first confirmed efficient ablation of YAP/TAZ in SCs by analyzing contralateral, intact nerves of iDKO mice (Figure 2B, 2F). We excluded mice with poor deletion (i.e., exhibiting YAP/TAZ in >20% SCs) from further analysis. Notably, pulse labeling with EdU indicated that the transected nerves of WT and iDKO contained similar numbers of dividing SCs in S phase (Figure 2C, 2G; 12.8% WT, 16.5% iDKO, p=0.0742). Numbers of Ki67+ proliferating SCs (Figure 2D, 2H; 40.5% WT, 40.4% iDKO, p=0.8760) and of total SCs (Figure 2E, 2I) were also similar in the transected nerves of WT and iDKO.

If adult SCs lacking YAP/TAZ in iDKO die or proliferate independently of axotomy, our analysis of injury-elicited SC proliferation might be confounded. To exclude this possibility, we examined contralateral, intact nerves of WT and iDKO mice at 12 dpi for SC proliferation and death (Figure 2-figure supplement 1A). Contralateral iDKO nerves contained neither EdU+ SCs (Figure 2-figure supplement 1B) nor apoptotic SCs, as assessed by TUNEL assays (Figure 2-figure supplement 1C) and caspase 3 staining (data not shown). We also found that SC numbers did not differ significantly from those in intact nerves of WT mice (Figure 2-figure supplement 1D, E). Collectively, these results strongly indicate that YAP/TAZ do not regulate SC proliferation after nerve injury.

SCs lacking YAP/TAZ convert to repair SCs and support axon regeneration

Next, we investigated if transdifferentiation to repair SCs proceeds normally in iDKO nerves after injury. We first examined expression of c-Jun, phosphorylated c-Jun, p75 and Oct-6 in repair SCs during nerve regeneration (Scherer et al., 1994; Parkinson et al., 2008; Arthur-Farraj et al., 2012; Fontana et al., 2012). Repair SC formation particularly depends on the upregulation of c-Jun, which promotes expression of regeneration-associated genes (RAG), such as p75 neurotrophin receptor (NTR) (Parkinson et al., 2008; Arthur-Farraj et al., 2012; Fontana et al., 2012). Immunohistochemical analysis of transected sciatic nerves at 5 dpi showed that WT and iDKO mice contained similar numbers of SCs expressing c-Jun (Figure 3A, 3E) or active pc-Jun (Figure 3B, 3F). There was minimal or no expression of c-Jun in contralateral, intact nerves of iDKO at 5 dpi (data not shown). We also found that p75 NTR expression was strongly upregulated in iDKO SCs, as in WT SCs (Figure 3C), and that Oct-6 expression in WT and iDKO SCs did not differ (Figure 3D, 3G).

SCs are essential for successful nerve regeneration (Scheib and Hoke, 2013; Jessen and Mirsky, 2016). As the definitive test of whether iDKO SCs convert normally to repair SCs, we next examined if the absence of YAP/TAZ in SCs impairs nerve regeneration. Because *Yap/Taz* iDKO mice die ~14 days after tamoxifen treatment (Grove et al., 2017), we crushed sciatic nerves and analyzed them on 12-13 dpi. To minimize variability, we crushed nerves at the same site close to the sciatic notch and analyzed nerve segments immunohistochemically or ultrastructurally at the same distance distal to the injury (Figure 4A). An anti-β3 tubulin antibody,

which identifies all axons, intensely labeled many axons that had regenerated through the ~1 cm long distal nerve stumps of iDKO mice (Figure 4B, 4D). These axons were as thick and numerous in iDKO as in WT nerves (Figure 4B, 4F, Figure 5-figure supplement 1). Similar numbers of axons were also present in contralateral intact nerves of WT and iDKO (Figure 4F), indicating that there was no axon degeneration in intact nerves of iDKO at 12-13 dpi.

To confirm these findings, we examined transverse nerve segments 5 mm distal to the injury by TEM. In this ultrastructural analysis, we took advantage of the fact that regenerating axons extend through the basal lamina (BL) tubes that surround SCs and their processes (Scheib and Hoke, 2013; Jessen and Mirsky, 2016). We found that the percentage of BL tubes containing axons (single or multiple) was similar in WT and iDKO nerves (Figure 4 E, 4G; WT, 86.6% vs. iDKO, 86.7%, p=0.9591). Furthermore, the percentage of BL tubes containing axons large enough to be myelinated (i.e., >1μm) did not differ (Figure 4H; WT, 62.4% vs. iDKO, 66.2%, p=0.3654). However, the large axons in iDKO nerves were more frequently accompanied by one or multiple, often thin, axons, which presumably represent transient collateral sprouts (e.g., Figure 4E-d, 4I; WT, 26.4% vs. iDKO, 51.3%, p=0.0015). Taken together, these results show that SCs lacking YAP/TAZ convert normally to repair SCs and support axon regeneration after injury.

YAP/TAZ are required for Schwann cells to myelinate regenerated axons

We have previously reported that developing SCs lacking YAP/TAZ arrest as promyelinating SCs, and are therefore unable to initiate myelin formation (Grove et al., 2017). To determine if adult SCs lacking YAP/TAZ can myelinate regenerating axons, we next analyzed the extent of myelination in the same iDKO nerves analyzed for axon regeneration. As expected, there was strong expression of myelin basic protein (MBP), a major structural component of the myelin sheath, in the crushed nerves of WT mice (Figure 5A, 5B). MBP immunoreactivity was also abundant in the contralateral, intact nerves of iDKO mice (Figure 5A), in which our previous ultrastructural analysis found segmental demyelination (Grove et al., 2017). In contrast, iDKO crushed nerves revealed remarkably little, if any, MBP immunoreactivity (Figure 5A, 5C, Figure 5-figure supplement 1). Consistent with this immunohistochemical analysis, semithin (Figure 5D) and ultrathin sections processed for EM (Figure 4E) revealed many myelinated axons in WT but

almost none in iDKO crushed nerves (Figure 5F, 5G). Moreover, iDKO SCs frequently surrounded and established 1:1 relationships with large axons, but none of these axons exhibited a myelin sheath (Figure 5D, 5E). These findings show that adult SCs lacking YAP/TAZ cannot initiate remyelination because they arrest at the promyelinating stage after injury.

YAP and TAZ are functionally redundant and required for optimal remyelination

Mindos et al. recently reported that expression of YAP, assessed by Western blotting, increases after nerve injury in mutant nerves lacking Merlin in SCs, but not in WT nerves, whereas TAZ increases in both WT and mutant nerves (Mindos et al., 2017). They also reported that elevated YAP levels prevent axon regeneration and remyelination, and that inactivation of YAP alone is sufficient to restore full functional recovery of the Merlin mutants (Mindos et al., 2017). These observations suggest that the function of TAZ in adult SCs differs from that of YAP. We next examined axon regeneration and remyelination when SCs express YAP but not TAZ. We reasoned that, if YAP prevents regeneration, regardless of expression levels, and if it differs functionally from TAZ, then we would find axon regeneration and remyelination to be poor.

Using a TAZ-selective tamoxifen inducible line to inactivate TAZ in SCs (*Plp1-creERT2*; $Yap^{+/+}$; $Taz^{fl/fl}$, hereafter *Taz* iKO), we crushed sciatic nerves unilaterally and compared the mutants to WT and *Yap/Taz* iDKO mice at 12 dpi. After confirming efficient inactivation of TAZ and no compensatory elevation of YAP levels in *Taz* iKO (Figure 6B), we used β3 tubulin to label axons and found that as many axons regenerated into the distal nerve stumps of *Taz* iKO, as of WT and *Yap/Taz* iDKO (data not shown). Ultrastructural analysis of nerve segments at 5 mm distal to the injury revealed many BL tubes containing single or multiple axons in *Taz* iKO, as in WT (Figure 6A). These axon-containing BL tubes were as numerous in iKO as in WT and iDKO (Figure 6C; WT, 86.6% vs. iDKO, 86.7% vs. *Taz* iKO, 87.8%; WT vs. iDKO, p=0.99; WT vs. iKO, p = 0.90; iDKO vs. iKO, p= 0.92). Counts of BL tubes containing axons large enough to be myelinated also did not differ (Figure 6D; WT, 62.4% vs. iDKO, 66.2% vs. *Taz* iKO, 73%; WT vs. iDKO, p=0.72; WT vs. iKO, p=0.52; iDKO vs. iKO, p=0.2). Therefore axons regenerated as robustly in *Taz* iKO as in WT and iDKO nerves, indicating that SCs expressing only YAP supported axon regeneration. We also found that, whereas iDKO nerves contained no myelinated axons (Figure 5D), myelinated axons were frequent in *Taz* iKO nerves (Figure 6A, 6E), and G-

ratios did not differ in *Taz* iKO and WT (Figure 6F), demonstrating that SCs expressing only YAP were capable of myelinating regenerated axons. Notably, however, a significantly smaller percentage of single axons were myelinated in Taz iKO than in WT (Figure 6E; WT, 69.6% vs. iDKO 1.3%, iKO, 42.3%; WT vs. iDKO, p=<0.0001; WT vs. iKO, p=0.0094; iDKO vs. iKO, p=0.0016), indicating that remyelination is less advanced in *Taz* iKO nerves which express only YAP in SCs. Taken together, these results show that YAP, at normal levels, does not prevent axon regeneration or remyelination after injury, and that both YAP and TAZ are required for optimal remyelination after injury.

Redifferentiation of Schwann cells lacking YAP/TAZ

We next investigated why SCs lacking YAP/TAZ fail to myelinate regenerated axons. Following axon regeneration, denervated SCs that have regained axon contacts downregulate dedifferentiation-associated genes while upregulating genes promoting differentiation (Stassart et al., 2013; Quintes et al., 2016; Wu et al., 2016). It is possible that iDKO SCs do not myelinate regenerated axons because their capacity to carry out one or both processes is defective. To test if iDKO SCs can correctly downregulate dedifferentiation-associated genes, we compared expression of c-Jun, Ki67 and Oct-6 by WT and iDKO SCs at 5 and 12 dpi after crush. The number of c-Jun+ SCs was markedly, but similarly, reduced in nerves of both WT and iDKO at 12 dpi (Figure 7A, E), and proliferating SCs were rare (Figure 7B, 7F). Oct-6 expression was also reduced in both WT and iDKO (Figure 7C, 7G), although it remained statistically higher in iDKO SCs, suggesting that both WT and iDKO SCs withdraw gradually from dedifferentiation.

Lastly, we examined expression of Krox20 (also known as Egr2), the master transcription factor that drives myelin gene expression (Topilko et al., 1994; Decker et al., 2006). Notably, whereas WT SCs upregulated Krox20 expression at 12 dpi, concomitant with remyelination, few if any iDKO SCs exhibited Krox20 immunoreactivity (Figure 7D, 7H). These results indicate that SCs fail to myelinate regenerated axons at least in part due to failure to upregulate Krox20. They also suggest that repair SCs lacking YAP/TAZ are capable of downregulating dedifferentiation genes but cannot upregulate myelin-associated genes.

DISCUSSION

Recent studies of SC-specific gene targeting consistently show that SCs lacking both YAP and TAZ are unable to proliferate properly and fail to myelinate developing peripheral nerves (Poitelon et al., 2016; Deng et al., 2017; Grove et al., 2017). It remains controversial, however, how YAP/TAZ loss results in complete amyelination of developing nerves and whether YAP/TAZ also play a role in myelin maintenance of adult nerves. Indeed, Poitelon et al., attributed developmental amyelination to the inability of immature SCs lacking YAP/TAZ to wrap around developing axons, a process called radial sorting (Feltri et al., 2016; Poitelon et al., 2016). In contrast, Grove et al. and Deng et al. attributed the myelination failure primarily to the inability of SCs to differentiate into myelinating SCs (Deng et al., 2017; Grove et al., 2017). Deng et al., however, disagreed with our view about the role of YAP/TAZ in maintaining adult myelination (Deng et al., 2017; Grove et al., 2017). These disagreements motivated the present study, which extends investigations of YAP/TAZ to their contribution to functional regeneration of peripheral nerves. We found that SCs lacking YAP/TAZ proliferate and wrap around regenerated axons, but then completely fail to remyelinate them. We also found that YAP/TAZ markedly disappear from denervated SCs, which we interpret as additional support for their role in myelin maintenance.

Using antibodies specifically immunolabeling YAP or YAP/TAZ, we found dramatic down-regulation of YAP/TAZ in denervated SCs followed by rapid upregulation in repair SCs, concomitant with axon degeneration and regeneration. Immunohistochemical identification of SC-selective YAP/TAZ was essential for detecting spatiotemporal regulation of YAP/TAZ. Indeed, we were only able to detect YAP/TAZ downregulation on Western blots when we used lysates prepared from nerves extensively perfused with saline, and from which the epi- and perineurium had been carefully removed. This procedure probably succeeded because it minimized the amount of YAP/TAZ present in cells other than SCs. Careful attention to YAP/TAZ expression in cells other than Schwann cells will help to resolve inconsistencies in earlier studies of YAP/TAZ expression in peripheral nerve.

YAP/TAZ are located in the nuclei of developing SCs, where they promote proliferation and differentiation (Poitelon et al., 2016; Deng et al., 2017; Grove et al., 2017). They are also nuclear and transcriptionally active in adult SCs that maintain the myelin sheath (Grove et al., 2017) and

that proliferate abnormally (Wu et al., 2018). It was therefore particularly intriguing to find that YAP/TAZ become undetectable in denervated SCs, and that they reappear as axons regenerate. This result has several important implications. First, it indicates that the nuclear localization of YAP/TAZ in mature SCs, and therefore the transcriptional regulation of SC proliferation and myelination by YAP/TAZ, is highly dependent on axons. It is also notable that YAP/TAZ appeared unchanged at 1 dpi, but had dramatically disappeared at 3 dpi, when axon degeneration was well underway (Beirowski et al., 2005; Gomez-Sanchez et al., 2015; Jang et al., 2016). This observation indicates that SC-axon interaction, likely contact-based, is essential for maintaining nuclear YAP/TAZ, at proper levels, in adult myelinating SCs.

Second, YAP/TAZ are potent stimulants of SC proliferation, but not an absolute requirement. We were surprised to find that YAP/TAZ are absent from denervated SCs that are actively proliferating at 3 dpi (Clemence et al., 1989), and that SC proliferation proceeds normally in *Yap/Taz* iDKO nerves after injury. Proliferation of mature SCs upon axon degeneration is therefore due to a YAP/TAZ-independent mechanism, in contrast to the proliferation of developing SCs, which is markedly reduced by YAP/TAZ inactivation (Clemence et al., 1989; Grove et al., 2017). This result is consistent with the notion that the mechanism for SC proliferation during development differs from that for proliferation after injury (Atanasoski et al., 2001; Atanasoski et al., 2008). However, abnormally high levels of YAP elicit excessive SC proliferation in Merlin mutants after nerve injury (Mindos et al., 2017), and YAP/TAZ overexpression induced by LATS1/2 inactivation elicits tumorigenic SC proliferation in adult nerves (Wu et al., 2018). These observations, together with our present results, indicate that YAP/TAZ are not normally involved in injury-elicited SC proliferation, but that, if overexpressed, YAP/TAZ can stimulate mature or denervated SCs to proliferate. It is also noteworthy that YAP/TAZ inactivation markedly reduces, but does not completely prevent, proliferation of developing SCs (Deng et al., 2017; Grove et al., 2017). We suggest, therefore, that YAP/TAZ, although not absolutely required, can powerfully stimulate developing and adult SCs to proliferate at all stages.

Third, YAP/TAZ in adult SCs function primarily to maintain myelination, which may explain why they are removed completely from denervated SCs. Tumorigenic proliferation of adult SCs

associated with abnormally increased YAP/TAZ levels (Wu et al., 2018) suggests the importance of maintaining proper levels of YAP/TAZ, but it does not explain why denervated SCs must lose YAP/TAZ completely. We attribute the requirement for complete loss to the pivotal role of YAP/TAZ in myelin maintenance by adult SCs (Grove et al., 2017). We previously demonstrated that YAP/TAZ are nuclear in myelinating, but not in non-myelinating, SCs, and that inducible deletion of YAP/TAZ elicits demyelination of adult intact nerve (Grove et al., 2017). If YAP/TAZ indeed maintain myelination and act by promoting transcription of Krox20 and other myelin genes, then sustaining YAP/TAZ would counteract demyelination and dedifferentiation of SCs after injury. Conversely, their absence would promote downregulation of myelin genes, facilitating demyelination and formation of repair SCs. In accordance with these ideas, transcription of Krox20 and other myelin genes remains robust in SCs up until 2 dpi, but is downregulated by 3 dpi (Arthur-Farraj et al., 2017), concomitant with the dramatic disappearance of YAP/TAZ observed in the present study. This proposed scenario, which emphasizes that YAP/TAZ play a passive role in Wallerian degeneration, predicts that SCs do not require YAP/TAZ to dedifferentiate, proliferate, or transdifferentiate to repair SCs. Indeed, these processes proceed normally in *Yap/Taz* iDKO mice. However, iDKO SCs are capable of wrapping around large diameter single axons but fail to initiate myelination, which recapitulates the developmental phenotype of these mutant mice (Deng et al., 2017; Grove et al., 2017). We also found that YAP and TAZ are functionally redundant in remyelination, as in developmental myelination. These observations therefore identify myelin maintenance and restoration as the primary functions of YAP/TAZ in adult SCs under physiological conditions.

YAP upregulation in SCs lacking Merlin has recently been reported to decrease the regeneration-promoting ability of repair SCs, which prevents axon regeneration in Merlin mutants (Mindos et al., 2017). This study implicates YAP as an inhibitor of axon regeneration. Our study suggests that this inhibition is dose- and context-dependent. We observed that repair SCs rapidly upregulate YAP/TAZ as axons regenerate and that expression persists as regeneration continues. We also found that axon regeneration is as robust in *Taz* iKO and *Yap/Taz* iDKO as in WT, but not noticeably enhanced. Given that YAP is not compensatorily upregulated in *Taz* iKO (Figure 6B), these results show that normal levels of YAP does not prevent axon regeneration. However, overly robust upregulation of YAP, as in Merlin mutants (Mindos et al., 2017), may severely

compromise axon regeneration because excessive levels of YAP/TAZ alter the growth-promoting ability of SCs and/or cause their tumorigenic proliferation.

The present study, together with earlier work, indicates that the levels of YAP/TAZ are a critical determinant of their function in adult SCs. Optimal levels of YAP/TAZ promote myelin formation, maintenance and remyelination, whereas their absence promotes demyelination. Contrarily, excessive levels of YAP/TAZ promote pathological SC proliferation. Additional efforts to confirm this notion and to understand the mechanisms that tightly regulate nuclear levels of YAP/TAZ in SCs may generate new strategies for peripheral nerve repair.

MATERIALS AND METHODS

Animals

All surgical procedures and animal maintenance complied with the National Institute of Health guidelines regarding the care and use of experimental animals and were approved by the Institutional Animal Care and Use Committee of Temple University, Philadelphia, PA, USA. All mice were of either sex, and were maintained on the C57/BL6 background. *Plp1-creERT2*; $Yap^{fl/fl}$; $Taz^{fl/fl}$**,** *Plp1-creERT2*; $Yap^{+/+}$; $Taz^{fl/fl}$, *P0-cre*;$Yap^{fl/fl}$ and *P0-cre*; $Taz^{fl/fl}$ mice used in this study were generated and genotyped as described previously (Grove et al., 2017). C57BL/6J mice were used for immunohistochemical analysis of YAP/TAZ.

Tamoxifen administration

Tamoxifen or 4-hydroxytamoxifen (4-HT; Sigma) was injected into 6-8 week old *Yap/Taz* iDKO or *Taz* iKO mice, as described previously (Grove et al., 2017).

Nerve crush or transection

Sciatic nerves of right hindlimbs were crushed or transected 24 h after the final tamoxifen injection, using standard protocols (Son and Thompson, 1995). Briefly, a small skin incision was made in the posterior thigh and calf of the animals anesthetized by isoflurane. For crush, the sciatic nerve was crushed with a fine forceps (#5) for 10 seconds (3X) adjacent to the sciatic notch. The crush site was marked using charcoal-coated forceps, and the wound was closed. For

transection, the exposed sciatic nerve was ligated at two directly adjacent sites, then cut with iridectomy scissors between the ligated sites. Ligated proximal and distal nerve endings were then sewn to adjacent muscle to prevent regeneration of axons from the proximal to distal nerve stumps.

Western blotting

Mice were perfused with PBS, sciatic nerves removed, and epineurium and perineurium carefully stripped from the nerves. Western blotting followed the same procedure described previously (Grove et al., 2017), except for IRDye 680RD goat anti-mouse IgG (LiCor #926-68070; 1:10,000).

Immunohistochemistry

For immunostaining, sciatic nerves were removed, fixed and processed as previously described (Grove et al., 2017). After sciatic nerve crush, nerve segments containing proximal nerve, crush site and distal nerve were harvested. In some experiments, nerve segments 5 mm distal to the crush site were used, as stated in the text. Nerve sections were incubated with antibodies previously described (Grove et al., 2017), except for the following: rabbit anti-Krox20 (kind gift from Professor Dies Meijer, Edinburgh, UK; 1:4000), rabbit anti-Yap (Cell Signaling #14074; 1:200), goat anti-Sox10 (Santa Cruz #sc-17342; 1:200), goat anti-Sox10 (R&D Systems #AF-2864; 1:100), goat anti-p75 (Neuromics #GT15057; 1:400), rabbit anti-Ki67 (Abcam #ab15580; 1:1000), mouse anti-Tubulin β3 (clone Tuj1, Covance #MMS-435P; 1:1000), mouse anti-cJun (BD Biosciences #610326; 1:500), rabbit anti-cJun (CST #9165; 1:500), rabbit anti-phospho-cJun (CST #9261; 1:100).

Electron microscopy, histology and morphometry

Sciatic nerves were removed and immediately fixed in EM buffer, as previously described (Grove et al., 2017). After nerve crush or transection, a 5 mm piece of the nerve was taken immediately distal to the injury site. The proximal end of the section was nicked with a razor blade for orientation during embedding. Fixation was for 2 h at room temperature, followed by overnight at 4^0C, with rotation. Post-fixation processing, embedding, cutting, staining and image capture were as previously described. For crushed or transected nerves, 500 nm semi-thin and 70

nm ultra-thin transverse sections were cut from the segment 5 mm distal to the crush/transection site.

For analysis of axon regeneration and remyelination, 7500x TEM sections were examined. This magnification allowed unambiguous identification of basal lamina tubes through which axons regenerate. Multiple non-overlapping images were taken for each section, such that all regions of each section were sampled. Image J was used for image analysis. After counting the total number of basal lamina (BL) tubes per image, we next counted the number of BL tubes in the following categories: contains no axon(s); contains axon(s); contains at least 1 axon > 1μm in diameter; contains a single axon > 1μm in diameter; contains a myelinated axon. This procedure enabled us to calculate the percentage of BL tubes in each category. Using an ImageJ G-ratio calculator plug-in, G ratios for each genotype were calculated in 2 different ways: (1) All single large axons were counted, whether or not they were myelinated; (2) Only myelinated axons were counted.

Data Analysis

In each experiment, data collection and analysis were performed identically, regardless of mouse genotype. Data are presented as mean +/- SEM. Statistical analysis was done using 2-way ANOVA with either Sidak's or Tukey's multiple comparison tests, one-way ANOVA with Tukey's multiple comparison test, or unpaired Student's t-test, according to the number of samples and the analysis of mice at multiple ages. Sample sizes were similar to those employed in the field and are indicated in the main text, methods or figure legends. Data distribution was assumed to be Gaussian, but was not formally tested, and $P< 0.05$ was considered significant.

ACKNOWLEDGMENTS

We thank Alan Tessler and members of the Son laboratory for critical reading of the manuscript. We thank Dr. Hyukmin Kim for intraperitoneal injection, Dr. Eric Olson for Yap and Taz floxed mice, Drs. Ueli Suter and Kelly Monk for Plp-creERT2 mice. Plp-creERT2 mice were generated by Dr. Ueli Suter using a patented Cre-ERT2 construct developed by Dr. Pierre Chambon at GIE-CERBM. This paper is dedicated to the memory of Dr. Wesley Thompson who revealed the pivotal roles of terminal Schwann cells in forming and restoring nerve-muscle connection.

COMPETING INTERESTS

The authors declare no competing financial interests.

AUTHOR CONTRIBUTIONS

M.G. and Y-J.S. designed and conceived the study. H.L. performed the surgical and light microscopic experiments presented in Figures 1, 4 and 5. M.G. performed the rest of the light microscopic, biochemical, and ultrastructural experiments. Y-J.S. wrote the manuscript.

FUNDINGS

This work was supported by grants from Shriners Hospitals for Children and NIH NINDS (NS105796 to Y-J.S.).

REFERENCES

Arthur-Farraj, P. J., Latouche, M., Wilton, D. K., Quintes, S., Chabrol, E., Banerjee, A., Woodhoo, A., Jenkins, B., Rahman, M., Turmaine, M., Wicher, G. K., Mitter, R., Greensmith, L., Behrens, A., Raivich, G., Mirsky, R., and Jessen, K. R. (2012). c-Jun reprograms Schwann cells of injured nerves to generate a repair cell essential for regeneration. *Neuron, 75*(4), 633-647. doi:10.1016/j.neuron.2012.06.021

Arthur-Farraj, P. J., Morgan, C. C., Adamowicz, M., Gomez-Sanchez, J. A., Fazal, S. V., Beucher, A., Razzaghi, B., Mirsky, R., Jessen, K. R., and Aitman, T. J. (2017). Changes in the Coding and Non-coding Transcriptome and DNA Methylome that Define the Schwann Cell Repair Phenotype after Nerve Injury. *Cell Rep, 20*(11), 2719-2734. doi:10.1016/j.celrep.2017.08.064

Atanasoski, S., Boentert, M., De Ventura, L., Pohl, H., Baranek, C., Beier, K., Young, P., Barbacid, M., and Suter, U. (2008). Postnatal Schwann cell proliferation but not myelination is strictly and uniquely dependent on cyclin-dependent kinase 4 (cdk4). *Mol Cell Neurosci, 37*(3), 519-527. doi:10.1016/j.mcn.2007.11.005

Atanasoski, S., Shumas, S., Dickson, C., Scherer, S. S., and Suter, U. (2001). Differential cyclin D1 requirements of proliferating Schwann cells during development and after injury. *Mol Cell Neurosci, 18*(6), 581-592. doi:10.1006/mcne.2001.1055

Beirowski, B., Adalbert, R., Wagner, D., Grumme, D. S., Addicks, K., Ribchester, R. R., and Coleman, M. P. (2005). The progressive nature of Wallerian degeneration in wild-type and slow Wallerian degeneration (WldS) nerves. *BMC Neurosci, 6*, 6. doi:10.1186/1471-2202-6-6

Clemence, A., Mirsky, R., and Jessen, K. R. (1989). Non-myelin-forming Schwann cells proliferate rapidly during Wallerian degeneration in the rat sciatic nerve. *J Neurocytol, 18*(2), 185-192.

Cotton, J. L., Li, Q., Ma, L., Park, J. S., Wang, J., Ou, J., Zhu, L. J., Ip, Y. T., Johnson, R. L., and Mao, J. (2017). YAP/TAZ and Hedgehog Coordinate Growth and Patterning in Gastrointestinal Mesenchyme. *Dev Cell, 43*(1), 35-47 e34. doi:10.1016/j.devcel.2017.08.019

Decker, L., Desmarquet-Trin-Dinh, C., Taillebourg, E., Ghislain, J., Vallat, J. M., and Charnay, P. (2006). Peripheral myelin maintenance is a dynamic process requiring constant Krox20 expression. *J Neurosci, 26*(38), 9771-9779. doi:10.1523/JNEUROSCI.0716-06.2006

Deng, Y., Wu, L. M. N., Bai, S., Zhao, C., Wang, H., Wang, J., Xu, L., Sakabe, M., Zhou, W., Xin, M., and Lu, Q. R. (2017). A reciprocal regulatory loop between TAZ/YAP and G-protein Galphas regulates Schwann cell proliferation and myelination. *Nat Commun, 8*, 15161. doi:10.1038/ncomms15161

Feltri, M. L., Poitelon, Y., and Previtali, S. C. (2016). How Schwann Cells Sort Axons: New Concepts. *Neuroscientist, 22*(3), 252-265. doi:10.1177/1073858415572361

Fernando, R. N., Cotter, L., Perrin-Tricaud, C., Berthelot, J., Bartolami, S., Pereira, J. A., Gonzalez, S., Suter, U., and Tricaud, N. (2016). Optimal myelin elongation relies on YAP activation by axonal growth and inhibition by Crb3/Hippo pathway. *Nat Commun, 7*, 12186. doi:10.1038/ncomms12186

Fex Svennigsen, A., and Dahlin, L. B. (2013). Repair of the Peripheral Nerve-Remyelination that Works. *Brain Sci, 3*(3), 1182-1197. doi:10.3390/brainsci3031182

Fontana, X., Hristova, M., Da Costa, C., Patodia, S., Thei, L., Makwana, M., Spencer-Dene, B., Latouche, M., Mirsky, R., Jessen, K. R., Klein, R., Raivich, G., and Behrens, A. (2012). c-Jun in Schwann cells promotes axonal regeneration and motoneuron survival via paracrine signaling. *J Cell Biol, 198*(1), 127-141. doi:10.1083/jcb.201205025

Gaudet, A. D., Popovich, P. G., and Ramer, M. S. (2011). Wallerian degeneration: gaining perspective on inflammatory events after peripheral nerve injury. *Journal of neuroinflammation, 8*, 110. doi:10.1186/1742-2094-8-110

Gomez-Sanchez, J. A., Carty, L., Iruarrizaga-Lejarreta, M., Palomo-Irigoyen, M., Varela-Rey, M., Griffith, M., Hantke, J., Macias-Camara, N., Azkargorta, M., Aurrekoetxea, I., De Juan, V. G., Jefferies, H. B., Aspichueta, P., Elortza, F., Aransay, A. M., Martinez-Chantar, M. L., Baas, F., Mato, J. M., Mirsky, R., Woodhoo, A., and Jessen, K. R. (2015). Schwann cell autophagy, myelinophagy, initiates myelin clearance from injured nerves. *J Cell Biol, 210*(1), 153-168. doi:10.1083/jcb.201503019

Grove, M., Kim, H., Santerre, M., Krupka, A. J., Han, S. B., Zhai, J., Cho, J. Y., Park, R., Harris, M., Kim, S., Sawaya, B. E., Kang, S. H., Barbe, M. F., Cho, S. H., Lemay, M. A., and

Son, Y. J. (2017). YAP/TAZ initiate and maintain Schwann cell myelination. *Elife, 6*. doi:10.7554/eLife.20982

Jang, S. Y., Shin, Y. K., Park, S. Y., Park, J. Y., Lee, H. J., Yoo, Y. H., Kim, J. K., and Park, H. T. (2016). Autophagic myelin destruction by Schwann cells during Wallerian degeneration and segmental demyelination. *Glia, 64*(5), 730-742. doi:10.1002/glia.22957

Jessen, K. R., and Mirsky, R. (2016). The repair Schwann cell and its function in regenerating nerves. *J Physiol, 594*(13), 3521-3531. doi:10.1113/jp270874

Lopez-Anido, C., Poitelon, Y., Gopinath, C., Moran, J. J., Ma, K. H., Law, W. D., Antonellis, A., Feltri, M. L., and Svaren, J. (2016). Tead1 regulates the expression of Peripheral Myelin Protein 22 during Schwann cell development. *Hum Mol Genet*. doi:10.1093/hmg/ddw158

Mindos, T., Dun, X. P., North, K., Doddrell, R. D., Schulz, A., Edwards, P., Russell, J., Gray, B., Roberts, S. L., Shivane, A., Mortimer, G., Pirie, M., Zhang, N., Pan, D., Morrison, H., and Parkinson, D. B. (2017). Merlin controls the repair capacity of Schwann cells after injury by regulating Hippo/YAP activity. *J Cell Biol, 216*(2), 495-510. doi:10.1083/jcb.201606052

Moon, S., Yeon Park, S., and Woo Park, H. (2018). Regulation of the Hippo pathway in cancer biology. *Cell Mol Life Sci, 75*(13), 2303-2319. doi:10.1007/s00018-018-2804-1

Parkinson, D. B., Bhaskaran, A., Arthur-Farraj, P., Noon, L. A., Woodhoo, A., Lloyd, A. C., Feltri, M. L., Wrabetz, L., Behrens, A., Mirsky, R., and Jessen, K. R. (2008). c-Jun is a negative regulator of myelination. *J Cell Biol, 181*(4), 625-637. doi:10.1083/jcb.200803013

Poitelon, Y., Lopez-Anido, C., Catignas, K., Berti, C., Palmisano, M., Williamson, C., Ameroso, D., Abiko, K., Hwang, Y., Gregorieff, A., Wrana, J. L., Asmani, M., Zhao, R., Sim, F. J., Wrabetz, L., Svaren, J., and Feltri, M. L. (2016). YAP and TAZ control peripheral myelination and the expression of laminin receptors in Schwann cells. *Nat Neurosci, 19*(7), 879-887. doi:10.1038/nn.4316

Quintes, S., Brinkmann, B. G., Ebert, M., Frob, F., Kungl, T., Arlt, F. A., Tarabykin, V., Huylebroeck, D., Meijer, D., Suter, U., Wegner, M., Sereda, M. W., and Nave, K. A. (2016). Zeb2 is essential for Schwann cell differentiation, myelination and nerve repair. *Nat Neurosci*. doi:10.1038/nn.4321

Scheib, J., and Hoke, A. (2013). Advances in peripheral nerve regeneration. *Nat Rev Neurol, 9*(12), 668-676. doi:10.1038/nrneurol.2013.227

Scherer, S. S., Wang, D. Y., Kuhn, R., Lemke, G., Wrabetz, L., and Kamholz, J. (1994). Axons regulate Schwann cell expression of the POU transcription factor SCIP. *J Neurosci, 14*(4), 1930-1942.

Son, Y.-J., and Thompson, W. J. (1995). Schwann cell processes guide regeneration of peripheral axons. *Neuron, 14*, 125-132.

Stassart, R. M., Fledrich, R., Velanac, V., Brinkmann, B. G., Schwab, M. H., Meijer, D., Sereda, M. W., and Nave, K. A. (2013). A role for Schwann cell-derived neuregulin-1 in remyelination. *Nat Neurosci, 16*(1), 48-54. doi:10.1038/nn.3281

Stierli, S., Napoli, I., White, I. J., Cattin, A. L., Monteza Cabrejos, A., Garcia Calavia, N., Malong, L., Ribeiro, S., Nihouarn, J., Williams, R., Young, K. M., Richardson, W. D., and Lloyd, A. C. (2018). The regulation of the homeostasis and regeneration of peripheral nerve is distinct from the CNS and independent of a stem cell population. *Development, 145*(24). doi:10.1242/dev.170316

Topilko, P., Schneider-Maunoury, S., Levi, G., Baron-Van Evercooren, A., Chennoufi, A. B., Seitanidou, T., Babinet, C., and Charnay, P. (1994). Krox-20 controls myelination in the peripheral nervous system. *Nature, 371*(6500), 796-799. doi:10.1038/371796a0

Tricaud, N., and Park, H. T. (2017). Wallerian demyelination: chronicle of a cellular cataclysm. *Cell Mol Life Sci, 74*(22), 4049-4057. doi:10.1007/s00018-017-2565-2

Varelas, X. (2014). The Hippo pathway effectors TAZ and YAP in development, homeostasis and disease. *Development, 141*(8), 1614-1626. doi:10.1242/dev.102376

von Gise, A., Lin, Z., Schlegelmilch, K., Honor, L. B., Pan, G. M., Buck, J. N., Ma, Q., Ishiwata, T., Zhou, B., Camargo, F. D., and Pu, W. T. (2012). YAP1, the nuclear target of Hippo signaling, stimulates heart growth through cardiomyocyte proliferation but not hypertrophy. *Proc Natl Acad Sci U S A, 109*(7), 2394-2399. doi:10.1073/pnas.1116136109

Wang, J., Liu, S., Heallen, T., and Martin, J. F. (2018). The Hippo pathway in the heart: pivotal roles in development, disease, and regeneration. *Nat Rev Cardiol, 15*(11), 672-684. doi:10.1038/s41569-018-0063-3

Wu, L. M., Wang, J., Conidi, A., Zhao, C., Wang, H., Ford, Z., Zhang, L., Zweier, C., Ayee, B. G., Maurel, P., Zwijsen, A., Chan, J. R., Jankowski, M. P., Huylebroeck, D., and Lu, Q. R. (2016). Zeb2 recruits HDAC-NuRD to inhibit Notch and controls Schwann cell differentiation and remyelination. *Nat Neurosci*. doi:10.1038/nn.4322

Wu, L. M. N., Deng, Y., Wang, J., Zhao, C., Wang, J., Rao, R., Xu, L., Zhou, W., Choi, K., Rizvi, T. A., Remke, M., Rubin, J. B., Johnson, R. L., Carroll, T. J., Stemmer-Rachamimov, A. O., Wu, J., Zheng, Y., Xin, M., Ratner, N., and Lu, Q. R. (2018). Programming of Schwann Cells by Lats1/2-TAZ/YAP Signaling Drives Malignant Peripheral Nerve Sheath Tumorigenesis. *Cancer Cell, 33*(2), 292-308 e297. doi:10.1016/j.ccell.2018.01.005

Xin, M., Kim, Y., Sutherland, L. B., Murakami, M., Qi, X., McAnally, J., Porrello, E. R., Mahmoud, A. I., Tan, W., Shelton, J. M., Richardson, J. A., Sadek, H. A., Bassel-Duby, R., and Olson, E. N. (2013). Hippo pathway effector Yap promotes cardiac regeneration. *Proc Natl Acad Sci U S A, 110*(34), 13839-13844. doi:10.1073/pnas.1313192110

Yu, F. X., Zhao, B., and Guan, K. L. (2015). Hippo Pathway in Organ Size Control, Tissue Homeostasis, and Cancer. *Cell, 163*(4), 811-828. doi:10.1016/j.cell.2015.10.044

Zanconato, F., Cordenonsi, M., and Piccolo, S. (2016). YAP/TAZ at the Roots of Cancer. *Cancer Cell, 29*(6), 783-803. doi:10.1016/j.ccell.2016.05.005

Zhang, H., Deo, M., Thompson, R. C., Uhler, M. D., and Turner, D. L. (2012). Negative regulation of Yap during neuronal differentiation. *Dev Biol, 361*(1), 103-115. doi:10.1016/j.ydbio.2011.10.017

FIGURE LEGENDS

Figure 1. Axon-dependent localization of YAP/TAZ in the Schwann cell nucleus

YAP/TAZ expression in transected (A, B, C) or crushed (D, E, F) sciatic nerves of adult mice. Axons and Schwann cell (SC) nuclei are marked by neurofilament (NF) or Sox10, respectively. (A) A surgery schematic for nerve transection illustrated by a low-magnification, longitudinal section of a sciatic nerve at 12 dpi, immunostained for YAP and TAZ. Axon regeneration into the distal nerve stump was prevented by ligating the transected nerve stumps. (B) Dramatic loss of YAP/TAZ, concomitant with axon degeneration, in SC nuclei of transected nerves. (C) Cytoplasmic loss of phosphorylated YAP (p-YAP) in SCs of transected nerves. (D) A surgery schematic for nerve crush, which permits regeneration of axons into the distal nerve stump. Numerous SC nuclei exhibiting bright YAP/TAZ labeling are present in the distal nerve at 12 dpi. (E) Upregulation of YAP/TAZ, concomitant with axon regeneration, in SC nuclei of crushed nerves. (F) Western blotting of intact and crushed nerve lysates, showing transient loss of YAP and TAZ at 3 dpi in crushed sciatic nerves. Scale bars; 500μm (A, D), 20μm (B, C, E).

The following figure supplements are available for Figure 1.

Figure 1-figure supplement 1

Additional assessment of YAP expression in Schwann cells after nerve injury

(A, B) Quantification of the Western blot data (Figure 1F), showing that YAP protein levels remain low (A), whereas TAZ protein levels are transiently low (B), at 3 dpi in crushed sciatic nerve lysates. n=3 mice per experiment. n.s. = not-significant, *P < 0.05, **P < 0.01, ***P < 0.001, ****P < 0.0001, 2-way ANOVA. (C) Validation of a YAP-specific antibody. The antibody labels perineurial cells but not SC nuclei in intact sciatic nerves of *Yap* cKO (*P0-Cre*;

Yap$^{fl/fl}$; *Taz*$^{+/+}$, Upper panel), whereas it labels SC nuclei in *Taz* cKO mice (*P0-Cre*; *Yap*$^{+/+}$; *Taz*$^{fl/fl}$, Bottom panel). (D) Longitudinal sections of crushed nerves, showing up-regulation of YAP in SC nuclei at or after 6 dpi. Scale bars = 15μm (C, D).

Figure 2. YAP/TAZ are dispensable for Schwann cell proliferation after axotomy

(A) Schematic showing timeline of tamoxifen injection, sciatic nerve transection and sacrifice of adult WT or Yap/Taz iDKO. (B) Longitudinal sections of intact sciatic nerves showing efficient deletion of YAP/TAZ in iDKO. SC nuclei are marked by Sox10 (red). All cell nuclei are marked by DAPI (blue). (C) Longitudinal sections of transected nerves of WT or iDKO showing SCs in S-phase of the cell cycle marked by EdU (green). (D) Longitudinal sections of transected nerves of WT or iDKO showing proliferating SCs marked by Ki67 (green). (E) Transverse sections of transected nerves of WT or iDKO showing SCs marked by Sox10 (red). (F) Quantification of SCs expressing nuclear YAP/TAZ in intact sciatic nerves of WT or iDKO. n = 3 mice per genotype, **P < 0.01, unpaired Student's t-test. (G) Quantification of EdU+ SCs in transected nerves of WT or iDKO. n = 3 mice per genotype, P > 0.05. (H) Quantification of Ki67+ proliferating SCs in transected nerves of WT or iDKO. n = 3 mice per genotype, P > 0.05. (I) Quantification of Sox10+ SCs in transected nerves of WT or iDKO. n = 3 mice per genotype, P > 0.05. Scale bars = 30μm (B-E).

The following figure supplements are available for Figure 2.

Figure 2-figure supplement 1

No Schwann cell proliferation or death in intact nerves of *Yap/Taz* iDKO at 12 dpi

(A) Schematic showing experimental procedures analyzing contralateral intact nerves of WT or iDKO at 12 dpi. (B) Longitudinal sections showing absence of EdU+ SCs in S-phase in intact nerves of iDKO, as in WT. Asterisks denote EdU+ cells that are not SCs, as indicated by their lack of Sox10. (C) Longitudinal sections of contralateral intact nerves, showing absence of apoptotic SCs identified by FITC-dUTP incorporation in iDKO, as in WT. (D) Transverse sections of intact nerves, showing similar numbers of SCs (marked by Sox10) in intact nerves of WT and iDKO at 12 dpi. All nuclei are marked by DAPI. (E) Quantification of SCs in intact nerves of WT or iDKO, showing no significant difference. n = 3 mice per genotype. P > 0.05, unpaired Student's t-test. Scale bars = 50μm (B-D).

Figure 3. Schwann cells lacking YAP/TAZ transdifferentiate into repair Schwann cells

Longitudinal sections of transected nerves of WT and *Yap/Taz* iDKO immunostained by various markers of growth-promoting repair SCs, 5 days after sciatic nerve transection. SCs are marked by Sox10 (red). (A) Representative sections showing upregulation of c-Jun in iDKO SCs, as in WT SCs. (B) Upregulation of active phospho-S73 c-Jun in iDKO SCs, as in WT. (C) Upregulation of p75 in iDKO SCs, as in WT SCs. (D) Upregulation of Oct-6 in iDKO SCs, as in WT SCs. (E) Quantification of c-Jun+ SCs in WT and iDKO. n = 3 mice per genotype. P> 0.05, unpaired Student's t-test. (F) Quantification of pc-Jun+ SCs in WT and iDKO. n = 3 mice per genotype. *P = 0.0145, unpaired Student's t-test. (G) Quantification of Oct-6+ SCs in WT and iDKO. n = 3 mice per genotype. P > 0.05, unpaired Student's t-test. Scale bars = 30μm (A-D).

Figure 4. Schwann cells lacking YAP/TAZ support axon regeneration

(A) Schematic showing relative locations and sizes of the distal nerve segments used for ultrastructural or light microscopic analysis of axon regeneration in WT or Yap/Taz iDKO, 12-13 days after nerve crush. (B) Low magnification views of longitudinal sections of ~5 mm long nerve segments distal to the crush site, showing regenerated axons in iDKO as abundant as in WT. Axons are marked by TuJ1. (C, D) High magnification views of boxed area in (B), ~8mm distal to the crush site. (E) Low and high magnification views of TEM, taken at 5mm distal to the crush site, showing numerous axons that regenerated within basal lamina tubes in iDKO, as in WT. 'ax' denotes an axon. Numerous axons are large (>1μm) but unmyelinated in iDKO. Examples of single large myelinated axons in WT (E-a, E-b), single large unmyelinated axon in iDKO (E-c) and axon bundles containing a large unmyelinated axon in iDKO (E-d). (F) Quantification of the axon density in intact and crushed nerves of WT and iDKO, n = 3 mice per genotype. P > 0.05, unpaired Student's t-test. (G) Quantification of the percentage of BL tubes containing axons in crushed nerves of WT and iDKO, n = 3 mice per genotype, P > 0.05, unpaired Student's t-test. (H) Quantification of the percentage of BL tubes containing at least one axon > 1μm in diameter, in crushed nerves of WT and iDKO. n = 3 mice per genotype. P > 0.05, unpaired Student's t-test. (I) Quantification of the percentage of BL tubes containing multiple axons, at least one of which is > 1μm in diameter, in crushed nerves of WT and iDKO.

n = 3 mice per genotype, **P < 0.01, unpaired Student's t-test. Scale bars = 500μm (B), 100μm (C, D), 2μm (E).

Figure 5. Schwann cells lacking YAP/TAZ fail to myelinate regenerated axons

Ultrastructural and light microscopic analyses of remyelination in distal nerves of WT or Yap/Taz iDKO, 12-13 days after nerve crush. (A) Low magnification views of longitudinal sections of intact or crushed nerves of WT and iDKO, showing no myelination of regenerated axons in crushed nerves of iDKO as indicated by the lack of MBP immunostaining. Refer to Figure 4B for robustly regenerated axons in the same iDKO mouse. (B, C) High magnification views of boxed area in (A), showing abundantly regenerated axons in crushed nerves of both WT (B) and iDKO (C). Note that regenerated axons in iDKO are not myelinated. Axons and myelin are marked by TuJ1 and MBP, respectively. (D) Semi-thin sections stained with toluidine blue showing numerous myelinated axons in crushed nerves of WT but not in iDKO. (E) TEM images of representative single large axons, myelinated in WT (left panel) but unmyelinated in iDKO (right panel). (F) Quantification of the percentage of single axons that are myelinated. n = 3 mice per genotype, ****P < 0.0001, unpaired Student's t-test. (G) G-ratio in WT and iDKO. Myelinated axons in WT are compared to unmyelinated single axons in iDKO. n = 3 mice per genotype, ***P < 0.001, unpaired Student's t-test. Scale bars = 500μm (A), 100μm (B, C), 10μm (D), 2μm (E).

The following figure supplements are available for Figure 5.

Figure 5-figure supplement 1

Additional images of axon regeneration and remyelination in WT and *Yap/Taz* iDKO

High magnification views of longitudinal sections of intact or crushed nerves of WT and iDKO, 12-13 days after nerve crush. Axons and myelin are marked by TuJ1 (green) and MBP (red), respectively. Numerous axons regenerated in crushed nerves of iDKO, as in WT, but they are unmyelinated. Myelin remains abundant, as indicated by abundant MBP, in contralateral intact nerves of iDKO at 12-13 dpi. Scale bar = 50μm

Figure 6. YAP/TAZ are redundant and required for optimal remyelination

Comparative analysis of axon regeneration and remyelination in WT and *Taz* iKO, 12-13 days after nerve crush. (A) Representative TEM images of WT and *Taz* iKO nerves, taken at 5mm distal to the crush site, showing numerous axons that regenerated within basal lamina tubes in *Taz* iKO, as in WT. 'ax' denotes a single axon. Some large axons are myelinated in Taz iKO. (B) Western blotting of sciatic nerve lysates, showing markedly reduced TAZ in *Taz* iKO, whereas YAP levels remain unchanged. YAP band is tighter and faster migrating in *Taz* iKO, than in WT, indicative of reduced phosphorylation. (C) Quantification of the percentage of BL tubes containing axons of any diameter in WT, *Taz* iKO and *Yap/Taz* iDKO nerves. n = 3 mice per genotype: WT vs. iDKO, P = 0.99; WT vs. iKO, P =0.90; iDKO vs. *Taz* iKO, P = 0.92, all non-significant, one-way ANOVA with Tukey's multiple comparison test. (D) Quantification of the percentage of BL tubes containing at least 1 axon larger than 1 μm in diameter in WT, *Taz* iKO and *Yap/Taz* iDKO nerves. n = 3 mice per genotype: WT vs. iDKO, P = 0.73; WT vs. iKO, P = 0.22; iDKO vs. iKO, P = 0.52, all non-significant, one-way ANOVA with Tukey's multiple comparison test. (E) Quantification of the percentage of single axons that are remyelinated in WT, *Taz* iKO and *Yap/Taz* iDKO nerves. n = 3 mice per genotype: WT vs. iDKO, ****P <0.0001; WT vs. iKO, **P = 0.0094; iDKO vs. *Taz* iKO, **P = 0.0016, one-way ANOVA with Tukey's multiple comparison test. (F) G-ratios of remyelinated axons in WT and *Taz* iKO nerves, compared to unmyelinated axons in *Yap/Taz* iDKO nerve. WT and *Taz* iKO remyelinated axons have equivalent G-ratios. n = 3 mice per genotype, WT vs. iDKO, ****P < 0.0001; WT vs. iKO, non-significant, P = 0.0744; iDKO vs. iKO, ***P =0.0008, one-way ANOVA with Tukey's multiple comparison test. Scale bar = 2μm (A).

Figure 7. Redifferentiation of Schwann cells lacking YAP/TAZ

Longitudinal sections of crushed nerves of WT and *Yap/Taz* iDKO at 12 dpi, immunostained by various makers of SC dedifferentiation (c-Jun and Oct-6), proliferation (Ki67) and redifferentiation (Krox20). SCs are marked by Sox10. (A) Representative sections showing c-Jun+ SCs markedly reduced in iDKO, as in WT. (B) Representative sections showing rarely observed Ki67+, proliferating SCs in iDKO, as in WT. (C) Representative sections showing Oct-6+ SCs reduced in iDKO, as in WT. (D) Representative sections showing failed upregulation of Krox20 in iDKO SCs. (E) Quantitative comparison of c-Jun+ SCs at 5 and 12 dpi, showing similar downregulation of c-Jun in WT and iDKO SC. n=3 mice per genotype, **P < 0.01, 2-

way ANOVA (F) Quantitative comparison of Ki67+ SCs, showing similar reduction in proliferating SCs in WT and iDKO nerves between 5 dpi and 12 dpi. n=3 mice per genotype. ****P < 0.0001, 2-way ANOVA. (G) Quantitative comparison of Oct-6+ SCs, showing significant downregulation of Oct-6 in WT and iDKO SCs between 5 dpi and 12 dpi. n=3 mice per genotype. n.s. = not significant, *P < 0.01, ***P < 0.001, 2-way ANOVA. (H) Quantitative comparison of Krox20+ SCs, showing upregulation of Krox20 in WT SCs, but not in iDKO SCs between 5 dpi and 12 dpi. n=3 mice per genotype. ****P < 0.0001, 2-way ANOVA. Scale bar = 10μm (A-D).

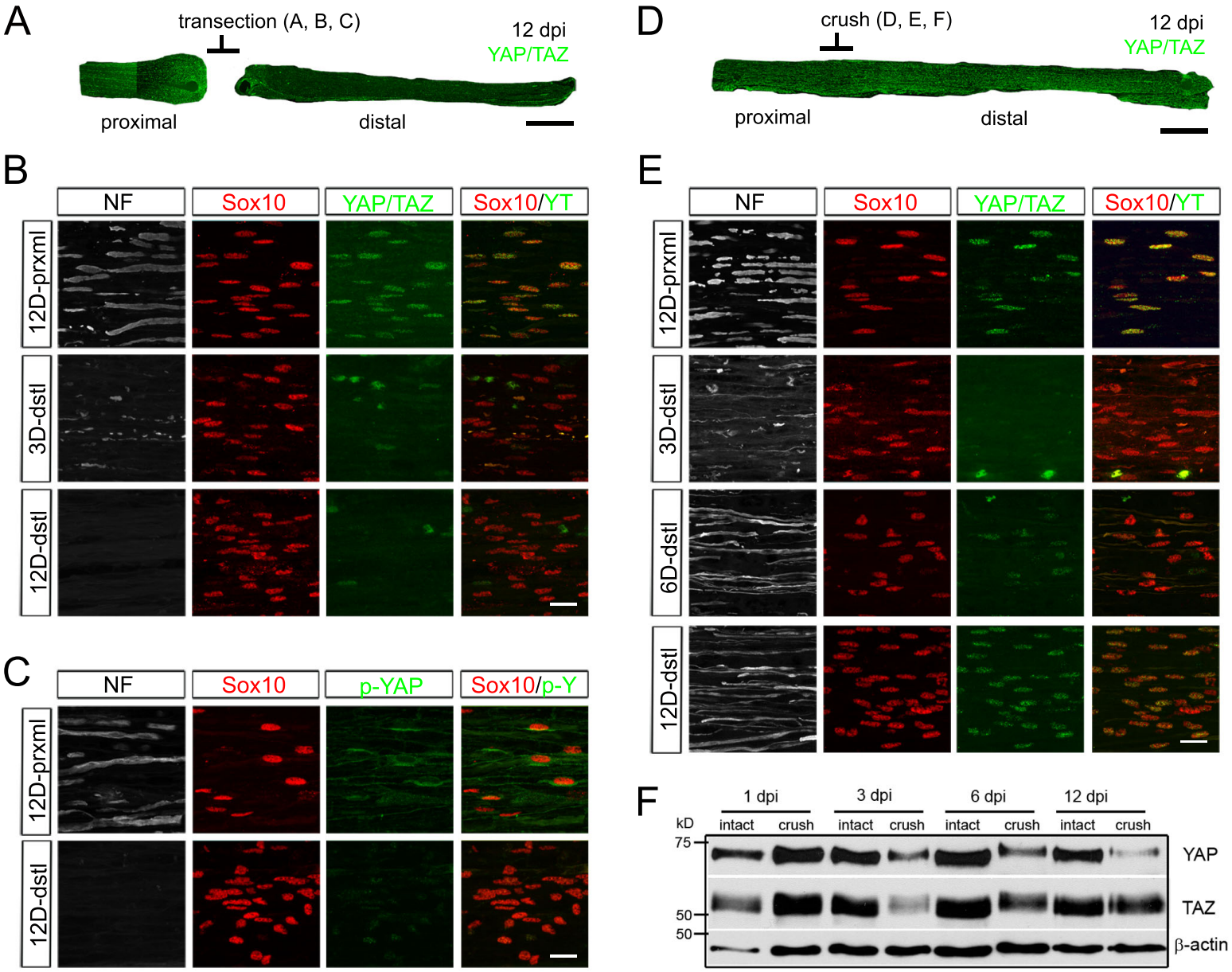

Figure 1. Axon-dependent localization of YAP/TAZ in the Schwann cell nucleus

YAP/TAZ expression in transected (A, B, C) or crushed (D, E, F) sciatic nerves of adult mice. Axons and Schwann cell (SC) nuclei are marked by neurofilament (NF) or Sox10, respectively. (A) A surgery schematic for nerve transection illustrated by a low-magnification, longitudinal section of a sciatic nerve at 12 dpi, immunostained for YAP and TAZ. Axon regeneration into the distal nerve stump was prevented by ligating the transected nerve stumps. (B) Dramatic loss of YAP/TAZ, concomitant with axon degeneration, in SC nuclei of transected nerves. (C) Cytoplasmic loss of phosphorylated YAP (p-YAP) in SCs of transected nerves. (D) A surgery schematic for nerve crush, which permits regeneration of axons into the distal nerve stump. Numerous SC nuclei exhibiting bright YAP/TAZ labeling are present in the distal nerve at 12 dpi. (E) Upregulation of YAP/TAZ, concomitant with axon regeneration, in SC nuclei of crushed nerves. (F) Western blotting of intact and crushed nerve lysates, showing transient loss of YAP and TAZ at 3 dpi in crushed sciatic nerves. Scale bars; 500μm (A, D), 20μm (B, C, E).

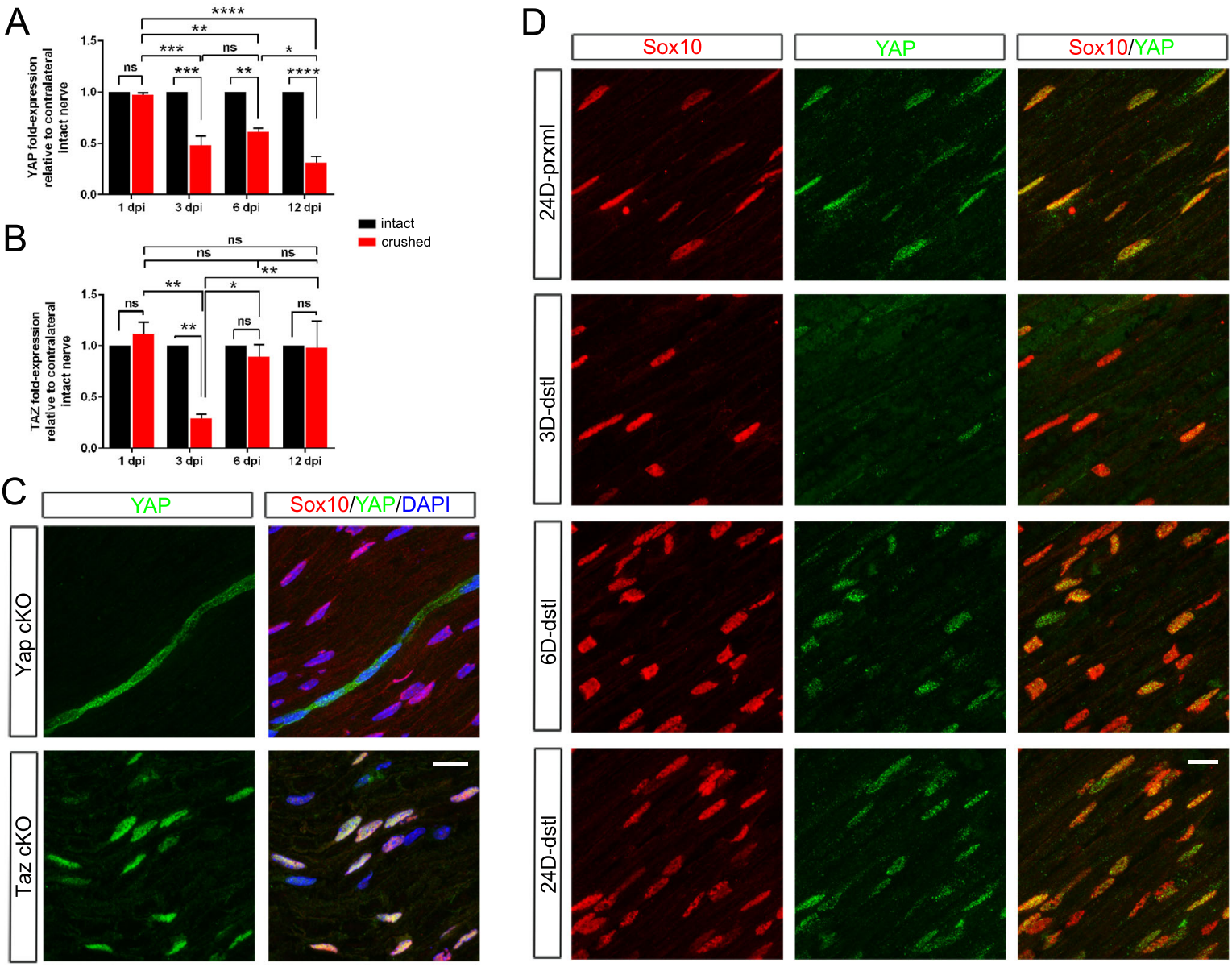

Figure 1-figure supplement 1

Additional assessment of YAP expression in Schwann cells after nerve injury

(A, B) Quantification of the Western blot data (Figure 1F), showing that YAP protein levels remain low (A), whereas TAZ protein levels are transiently low (B), at 3 dpi in crushed sciatic nerve lysates. n=3 mice per experiment. n.s. = not-significant, *P < 0.05, **P < 0.01, ***P < 0.001, ****P < 0.0001, 2-way ANOVA. (C) Validation of a YAP-specific antibody. The antibody labels perineurial cells but not SC nuclei in intact sciatic nerves of *Yap* cKO (*P0-Cre*; $Yap^{fl/fl}$; $Taz^{+/+}$, Upper panel), whereas it labels SC nuclei in *Taz* cKO mice (*P0-Cre*; $Yap^{+/+}$; $Taz^{fl/fl}$, Bottom panel). (D) Longitudinal sections of crushed nerves, showing up-regulation of YAP in SC nuclei at or after 6 dpi. Scale bars = 15μm (C, D).

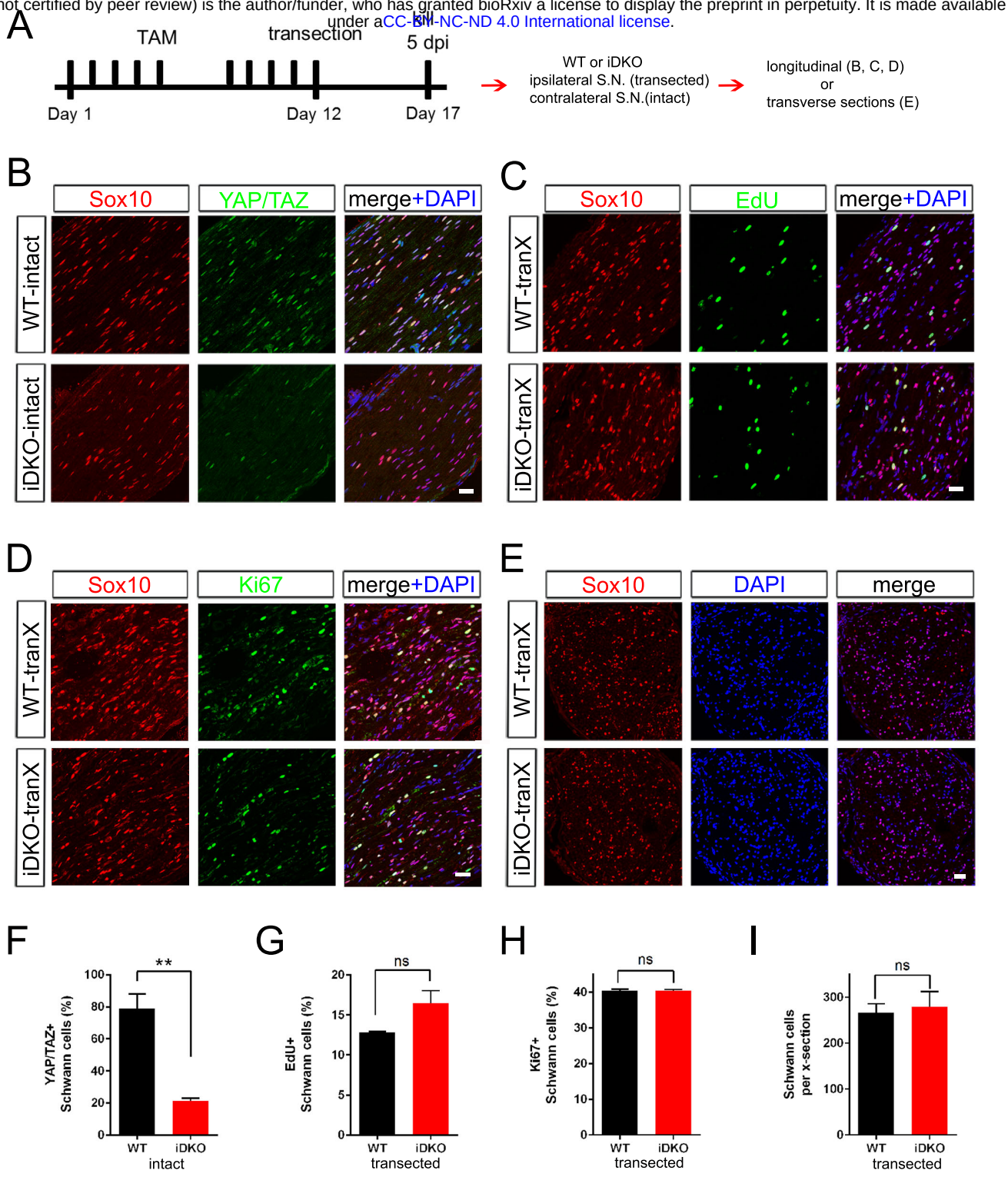

Figure 2. YAP/TAZ are dispensable for Schwann cell proliferation after axotomy

(A) Schematic showing timeline of tamoxifen injection, sciatic nerve transection and sacrifice of adult WT or Yap/Taz iDKO. (B) Longitudinal sections of intact sciatic nerves showing efficient deletion of YAP/TAZ in iDKO. SC nuclei are marked by Sox10 (red). All cell nuclei are marked by DAPI (blue). (C) Longitudinal sections of transected nerves of WT or iDKO showing SCs in S-phase of the cell cycle marked by EdU (green). (D) Longitudinal sections of transected nerves of WT or iDKO showing proliferating SCs marked by Ki67 (green). (E) Transverse sections of transected nerves of WT or iDKO showing SCs marked by Sox10 (red). (F) Quantification of SCs expressing nuclear YAP/TAZ in intact sciatic nerves of WT or iDKO. n = 3 mice per genotype, **P < 0.01, unpaired Student's t-test. (G) Quantification of EdU+ SCs in transected nerves of WT or iDKO. n = 3 mice per genotype, P > 0.05. (H) Quantification of Ki67+ proliferating SCs in transected nerves of WT or iDKO. n = 3 mice per genotype, P > 0.05. (I) Quantification of Sox10+ SCs in transected nerves of WT or iDKO. n = 3 mice per genotype, P > 0.05. Scale bars = 30μm (B-E).

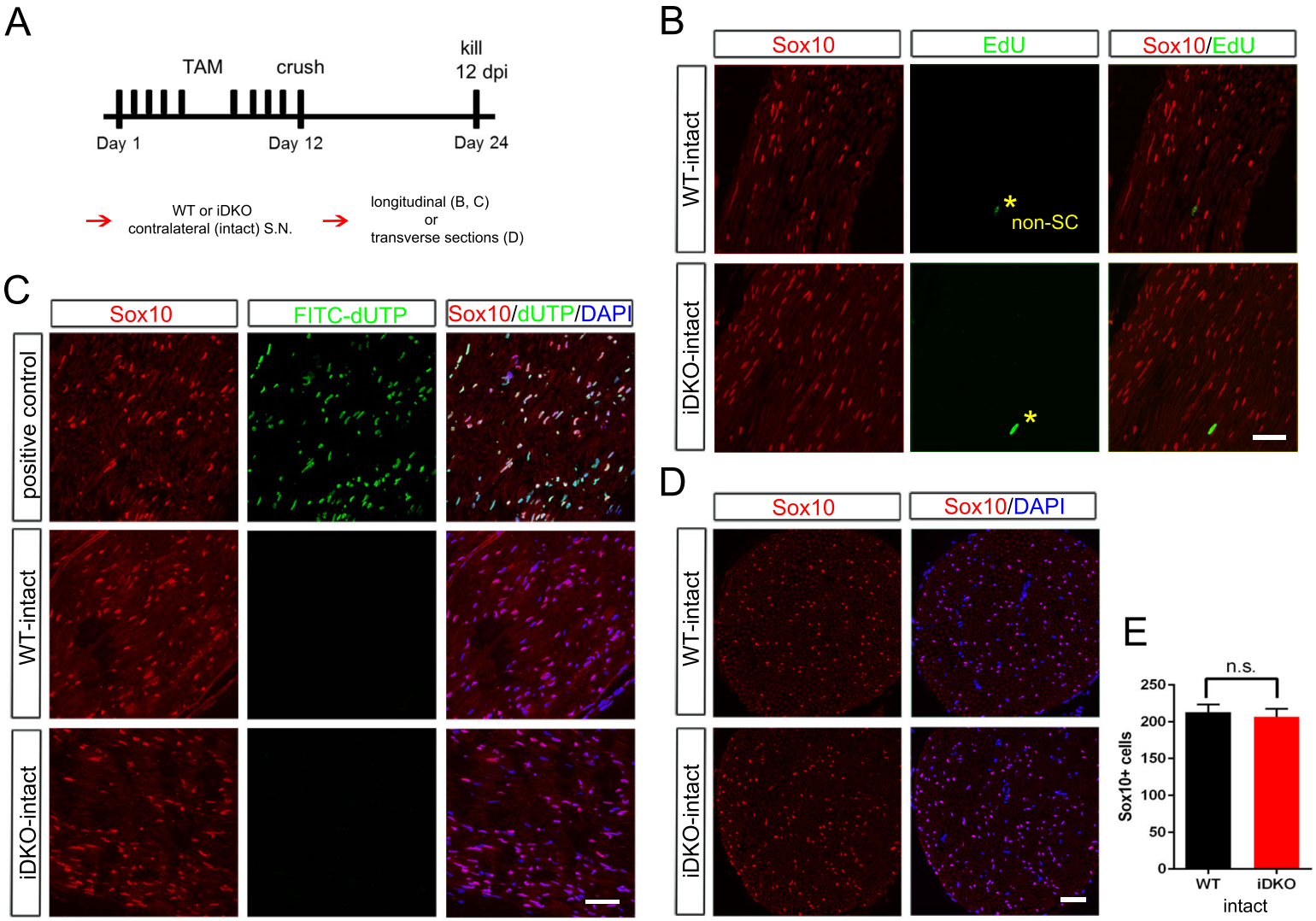

Figure 2-figure supplement 1

No Schwann cell proliferation or death in intact nerves of Yap/Taz iDKO at 12 dpi

(A) Schematic showing experimental procedures analyzing contralateral intact nerves of WT or iDKO at 12 dpi. (B) Longitudinal sections showing absence of EdU+ SCs in S-phase in intact nerves of iDKO, as in WT. Asterisks denote EdU+ cells that are not SCs, as indicated by their lack of Sox10. (C) Longitudinal sections of contralateral intact nerves, showing absence of apoptotic SCs identified by FITC-uUTP incorporation in iDKO, as in WT. (D) Transverse sections of intact nerves, showing similar numbers of SCs (marked by Sox10) in intact nerves of WT and iDKO at 12 dpi. All nuclei are marked by DAPI. (E) Quantification of SCs in intact nerves of WT or iDKO, showing no significant difference. n = 3 mice per genotype. $P > 0.05$, unpaired Student's t-test. Scale bars = 50μm (B-D).

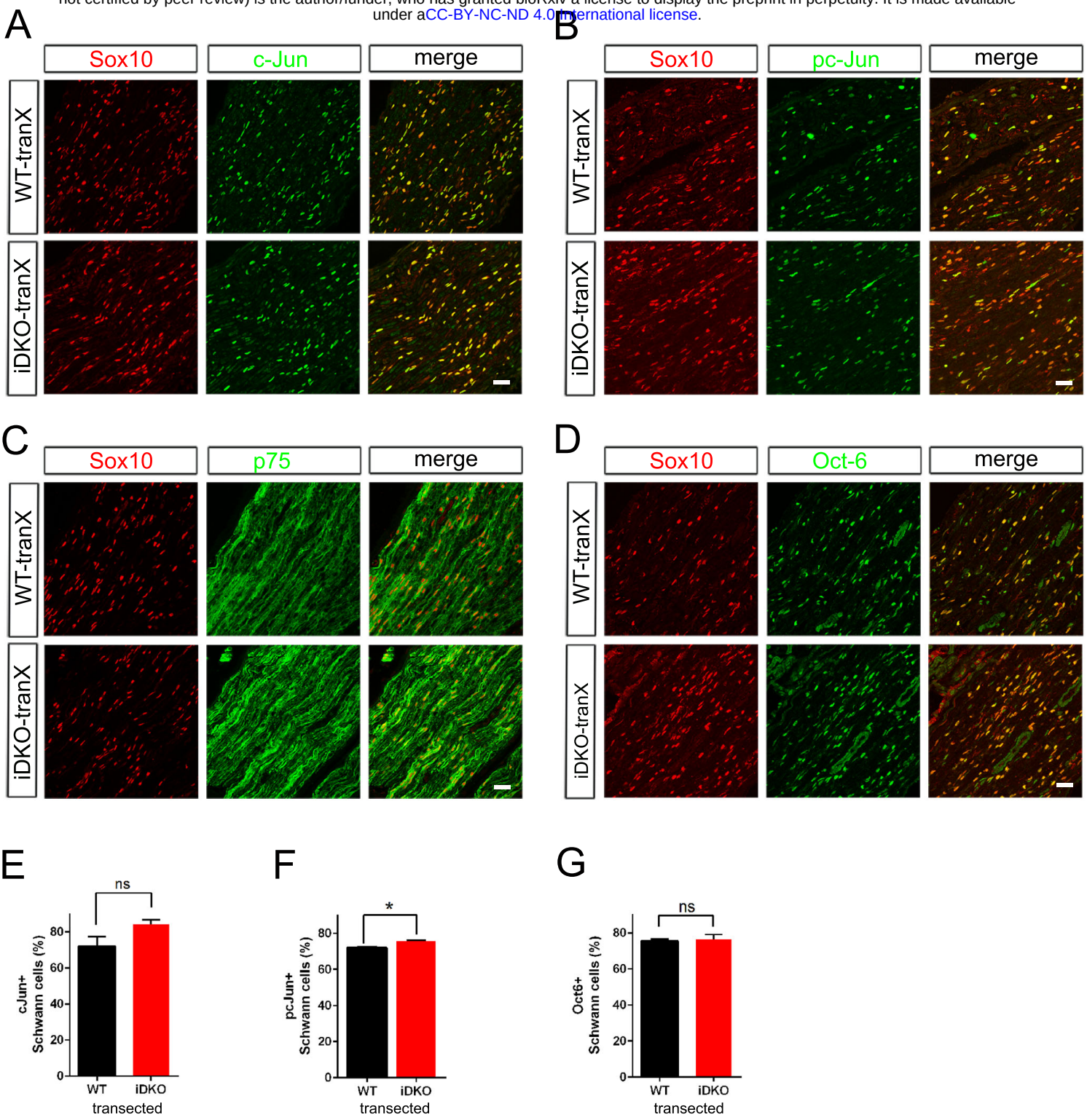

Figure 3. Schwann cells lacking YAP/TAZ transdifferentiate into repair Schwann cells
Longitudinal sections of transected nerves of WT and *Yap/Taz* iDKO immunostained by various markers of growth-promoting repair SCs, 5 days after sciatic nerve transection. SCs are marked by Sox10 (red). (A) Representative sections showing upregulation of c-Jun in iDKO SCs, as in WT SCs. (B) Upregulation of active phospho-S73 c-Jun in iDKO SCs, as in WT. (C) Upregulation of p75 in iDKO SCs, as in WT SCs. (D) Upregulation of Oct-6 in iDKO SCs, as in WT SCs. (E) Quantification of c-Jun+ SCs in WT and iDKO. n = 3 mice per genotype. P> 0.05, unpaired Student's t-test. (F) Quantification of pc-Jun+ SCs in WT and iDKO. n = 3 mice per genotype. *P = 0.0145, unpaired Student's t-test. (G) Quantification of Oct-6+ SCs in WT and iDKO. n = 3 mice per genotype. P > 0.05, unpaired Student's t-test. Scale bars = 30µm (A-D).

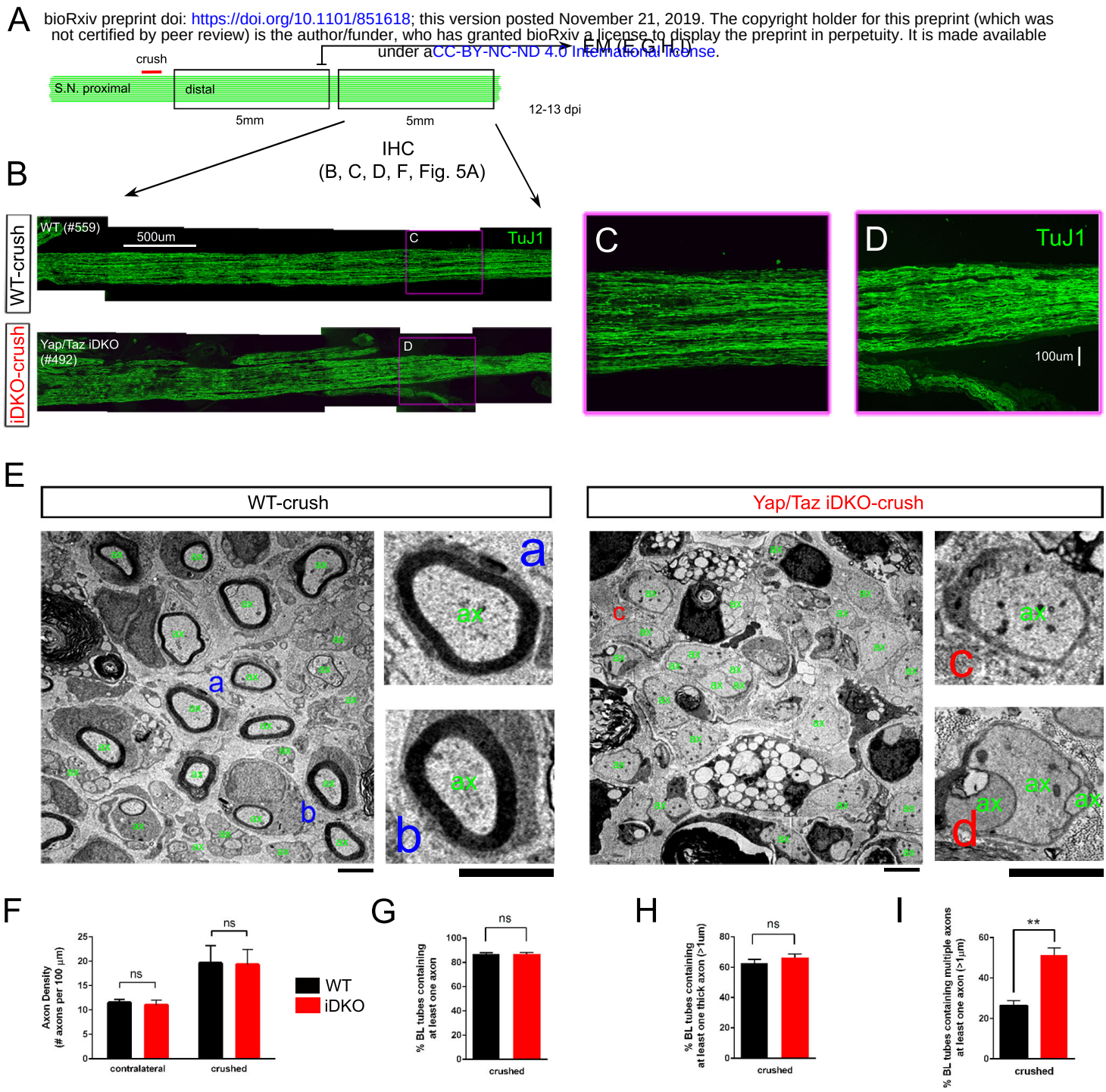

Figure 4. Schwann cells lacking YAP/TAZ support axon regeneration

(A) Schematic showing relative locations and sizes of the distal nerve segments used for ultrastructural or light microscopic analysis of axon regeneration in WT or Yap/Taz iDKO, 12-13 days after nerve crush. (B) Low magnification views of longitudinal sections of ~5 mm long nerve segments distal to the crush site, showing regenerated axons in iDKO as abundant as in WT. Axons are marked by TuJ1. (C, D) High magnification views of boxed area in (B), ~8mm distal to the crush site. (E) Low and high magnification views of TEM, taken at 5mm distal to the crush site, showing numerous axons that regenerated within basal lamina tubes in iDKO, as in WT. `ax' denotes an axon. Numerous axons are large (>1µm) but unmyelinated in iDKO. Examples of single large myelinated axons in WT (E-a, E-b), single large unmyelinated axon in iDKO (E-c) and axon bundles containing a large unmyelinated axon in iDKO (E-d). (F) Quantification of the axon density in intact and crushed nerves of WT and iDKO, n = 3 mice per genotype. P > 0.05, unpaired Student's t-test. (G) Quantification of the percentage of BL tubes containing axons in crushed nerves of WT and iDKO, n = 3 mice per genotype, P > 0.05, unpaired Student's t-test. (H) Quantification of the percentage of BL tubes containing at least one axon > 1µm in diameter, in crushed nerves of WT and iDKO. n = 3 mice per genotype. P > 0.05, unpaired Student's t-test. (I) Quantification of the percentage of BL tubes containing multiple axons, at least one of which is > 1µm in diameter, in crushed nerves of WT and iDKO. n = 3 mice per genotype, **P < 0.01, unpaired Student's t-test. Scale bars = 500µm (B), 100µm (C, D), 2µm (E).

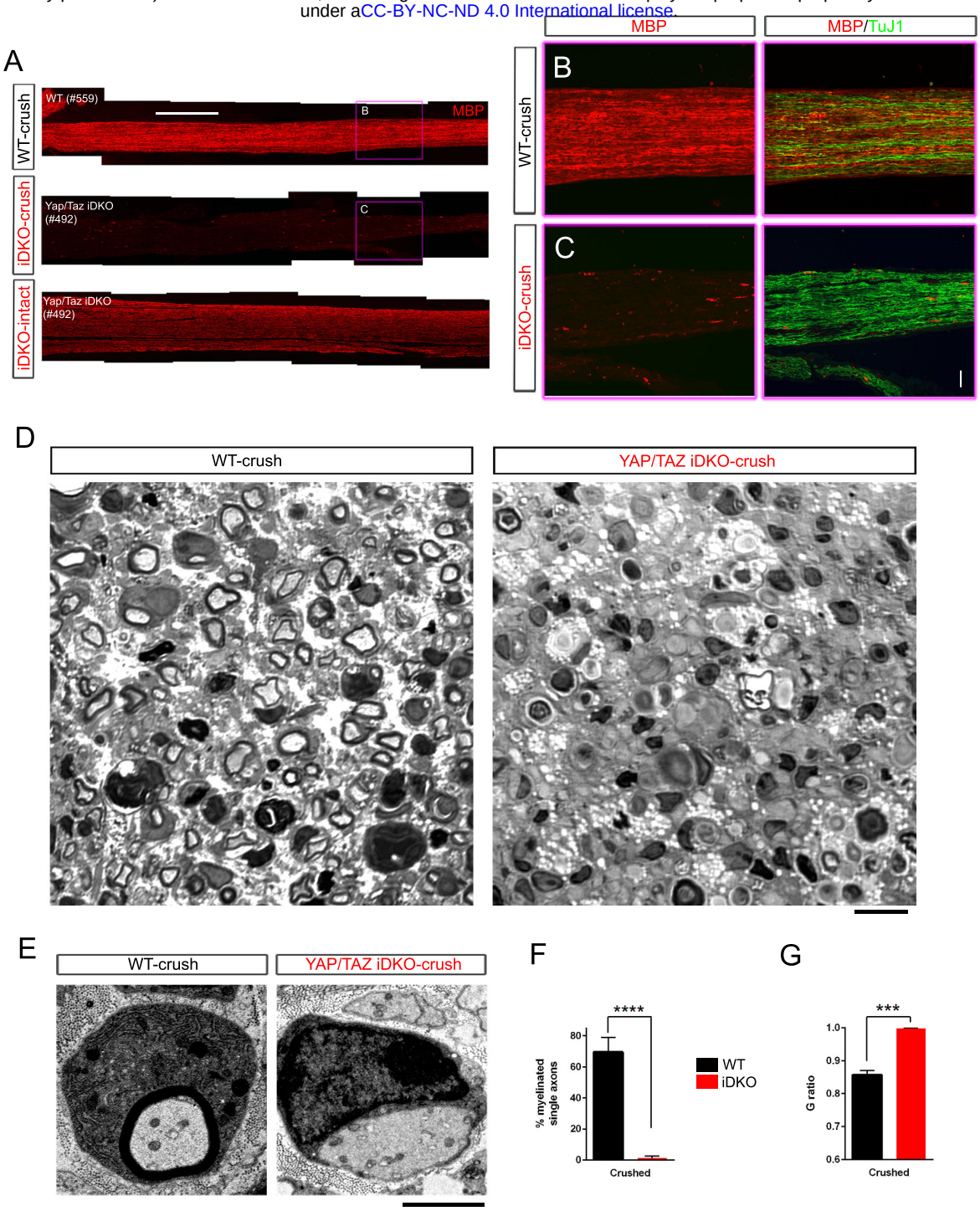

Figure 5. Schwann cells lacking YAP/TAZ fail to myelinate regenerated axons

Ultrastructural and light microscopic analyses of remyelination in distal nerves of WT or Yap/Taz iDKO, 12-13 days after nerve crush. (A) Low magnification views of longitudinal sections of intact or crushed nerves of WT and iDKO, showing no myelination of regenerated axons in crushed nerves of iDKO as indicated by the lack of MBP immunostaining. Refer to Figure 4B for robustly regenerated axons in the same iDKO mouse. (B, C) High magnification views of boxed area in (A), showing abundantly regenerated axons in crushed nerves of both WT (B) and iDKO (C). Note that regenerated axons in iDKO are not myelinated. Axons and myelin are marked by TuJ1 and MBP, respectively. (D) Semi-thin sections stained with toluidine blue showing numerous myelinated axons in crushed nerves of WT but not in iDKO. (E) TEM images of representative single large axons, myelinated in WT (left panel) but unmyelinated in iDKO (right panel). (F) Quantification of the percentage of single axons that are myelinated. n = 3 mice per genotype, ****P < 0.0001, unpaired Student's t-test. (G) G-ratio in WT and iDKO. Myelinated axons in WT are compared to unmyelinated single axons in iDKO. n = 3 mice per genotype, ***P < 0.001, unpaired Student's t-test. Scale bars = 500µm (A), 100µm (B, C), 10µm (D), 2µm (E).

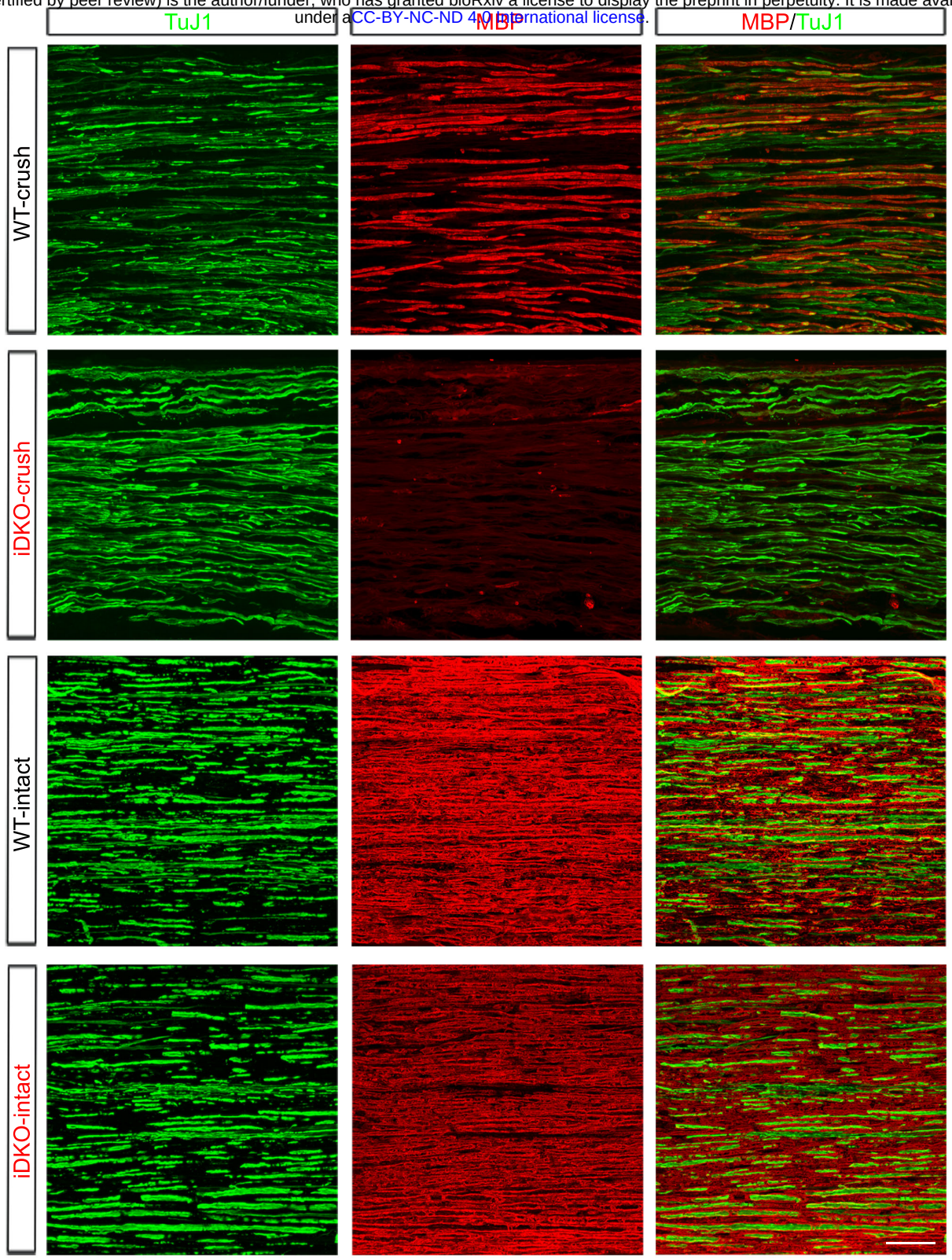

Figure 5-figure supplement 1

Additional images of axon regeneration and remyelination in WT and Yap/Taz iDKO

High magnification views of longitudinal sections of intact or crushed nerves of WT and iDKO, 12-13 days after nerve crush. Axons and myelin are marked by TuJ1 (green) and MBP (red), respectively. Numerous axons regenerated in crushed nerves of iDKO, as in WT, but they are unmyelinated. Myelin remains abundant, as indicated by abundant MBP, in contralateral intact nerves of iDKO at 12-13 dpi. Scale bar = 50μm

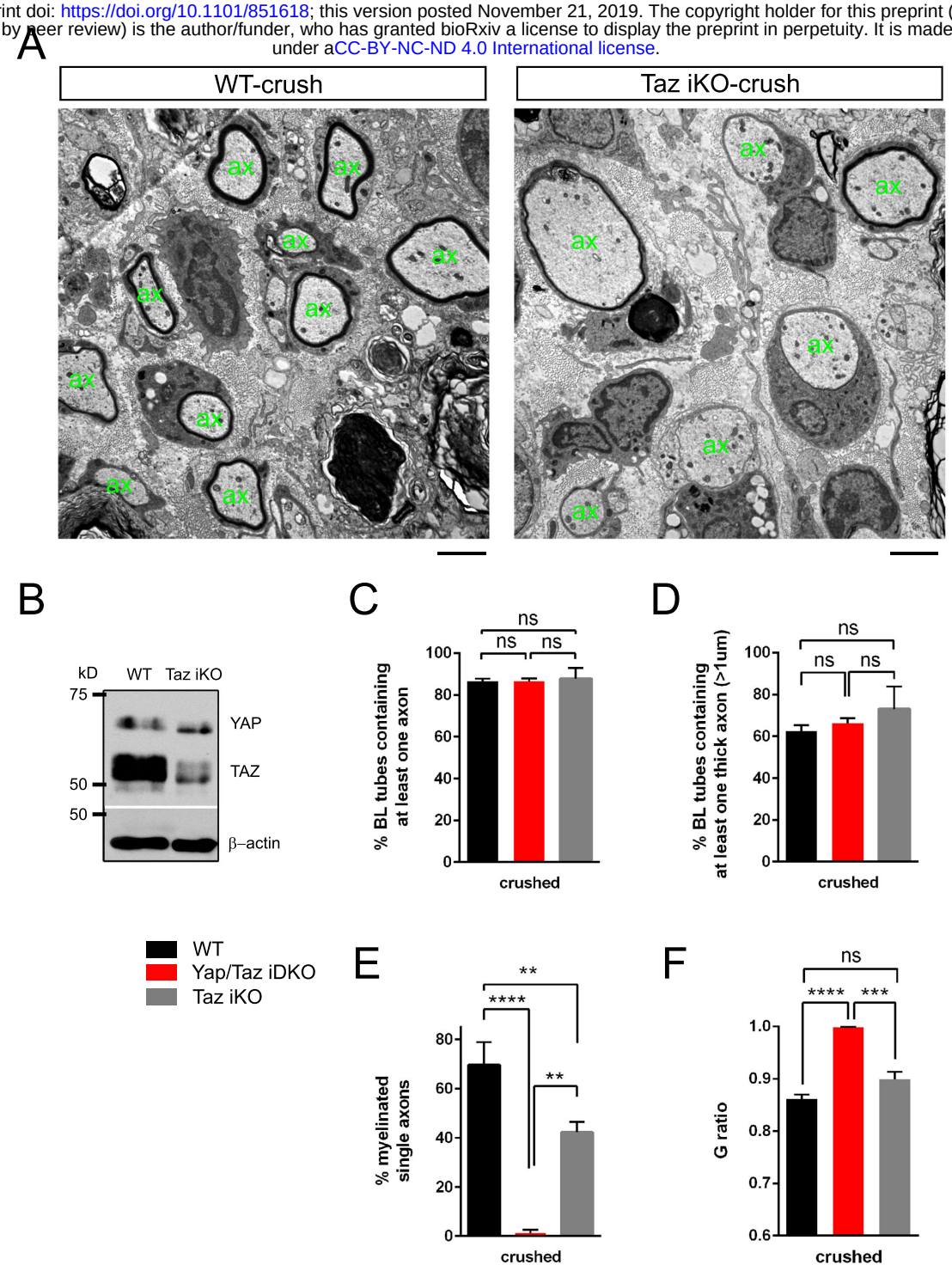

Figure 6. YAP/TAZ are redundant and required for optimal remyelination

Comparative analysis of axon regeneration and remyelination in WT and Taz iKO, 12-13 days after nerve crush. (A) Representative TEM images of WT and Taz iKO nerves, taken at 5mm distal to the crush site, showing numerous axons that regenerated within basal lamina tubes in Taz iKO, as in WT. `ax' denotes a single axon. Some large axons are myelinated in Taz iKO. (B) Western blotting of sciatic nerve lysates, showing markedly reduced TAZ in Taz iKO, whereas YAP levels remain unchanged. YAP band is tighter and faster migrating in Taz iKO, than in WT, indicative of reduced phosphorylation. (C) Quantification of the percentage of BL tubes containing axons of any diameter in WT, Taz iKO and Yap/Taz iDKO nerves. n = 3 mice per genotype: WT vs. iDKO, P = 0.99; WT vs. iKO, P =0.90; iDKO vs. Taz iKO, P = 0.92, all non-significant, one-way ANOVA with Tukey's multiple comparison test. (D) Quantification of the percentage of BL tubes containing at least 1 axon larger than 1 µm in diameter in WT, Taz iKO and Yap/Taz iDKO nerves. n = 3 mice per genotype: WT vs. iDKO, P = 0.73; WT vs. iKO, P = 0.22; iDKO vs. iKO, P = 0.52, all non-significant, one-way ANOVA with Tukey's multiple comparison test. (E) Quantification of the percentage of single axons that are remyelinated in WT, Taz iKO and Yap/Taz iDKO nerves. n = 3 mice per genotype: WT vs. iDKO, ****P <0.0001; WT vs. iKO, **P = 0.0094; iDKO vs. Tazi KO, **P = 0.0016, one-way ANOVA with Tukey's multiple comparison test. (F) G-ratios of remyelinated axons in WT and Taz iKO nerves, compared to unmyelinated axons in Yap/Taz iDKO nerve. WT and Taz iKO remyelinated axons have equivalent G-ratios. n = 3 mice per genotype, WT vs. iDKO, ****P < 0.0001; WT vs. iKO, non-significant, P = 0.0744; iDKO vs. iKO, ***P =0.0008, one-way ANOVA with Tukey's multiple comparison test. Scale bar = 2µm (A).

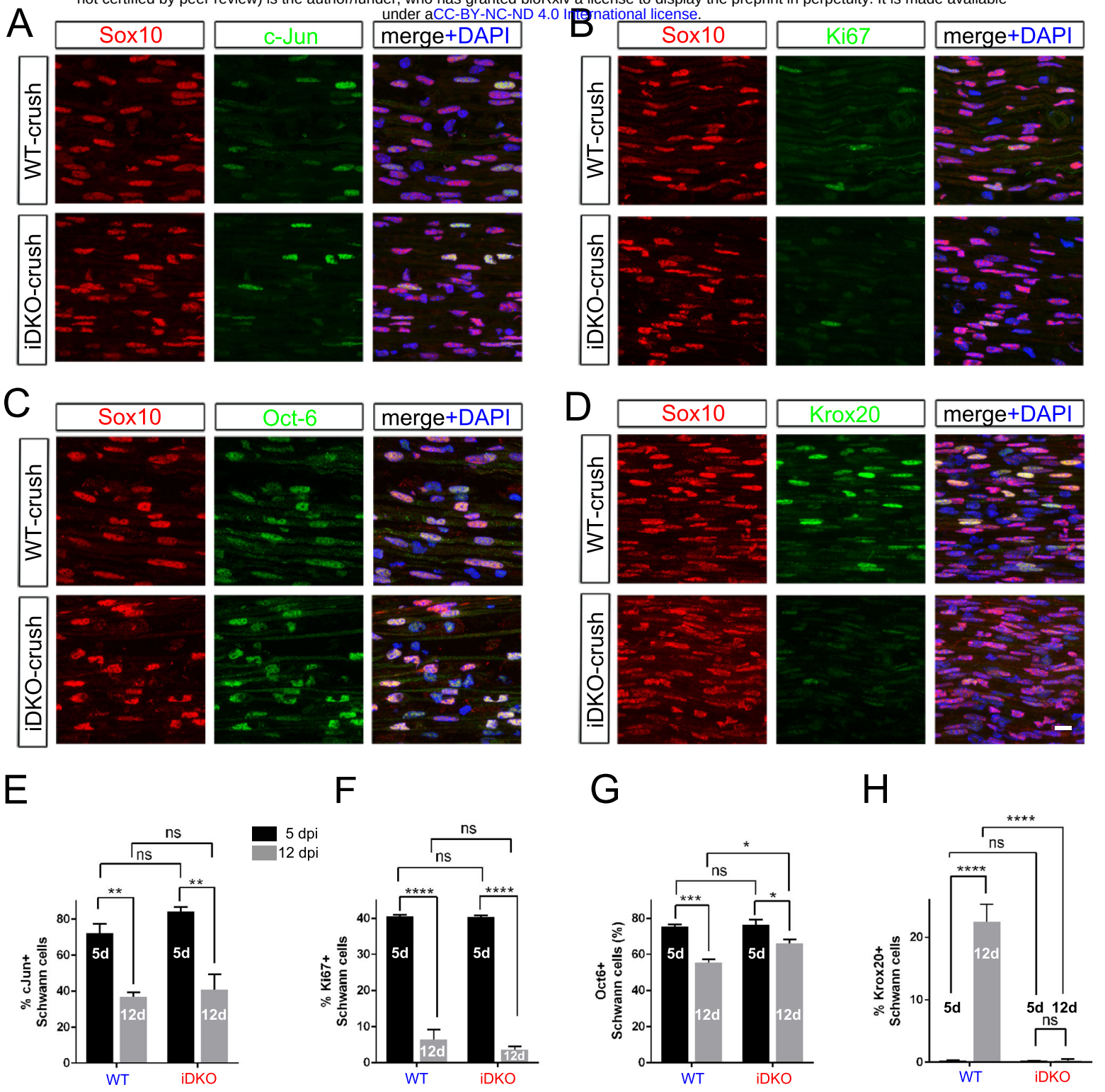

Figure 7. Redifferentiation of Schwann cells lacking YAP/TAZ

Longitudinal sections of crushed nerves of WT and *Yap/Taz* iDKO at 12 dpi, immunostained by various makers of SC dedifferentiation (c-Jun and Oct-6), proliferation (Ki67) and redifferentiation (Krox20). SCs are marked by Sox10. (A) Representative sections showing c-Jun+ SCs markedly reduced in iDKO, as in WT. (B) Representative sections showing rarely observed Ki67+, proliferating SCs in iDKO, as in WT. (C) Representative sections showing Oct-6+ SCs reduced in iDKO, as in WT. (D) Representative sections showing failed upregulation of Krox20 in iDKO SCs. (E) Quantitative comparison of c-Jun+ SCs at 5 and 12 dpi, showing similar downregulation of c-Jun in WT and iDKO SC. n=3 mice per genotype, $^{**}P < 0.01$, 2-way ANOVA (F) Quantitative comparison of Ki67+ SCs, showing similar reduction in proliferating SCs in WT and iDKO nerves between 5 dpi and 12 dpi. n=3 mice per genotype. $^{****}P < 0.0001$, 2-way ANOVA. (G) Quantitative comparison of Oct-6+ SCs, showing significant downregulation of Oct-6 in WT and iDKO SCs between 5 dpi and 12 dpi. n=3 mice per genotype. n.s. = not significant, $^{*}P < 0.01$, $^{***}P < 0.001$, 2-way ANOVA. (H) Quantitative comparison of Krox20+ SCs, showing upregulation of Krox20 in WT SCs, but not in iDKO SCs between 5 dpi and 12 dpi. n=3 mice per genotype. $^{****}P < 0.0001$, 2-way ANOVA. Scale bar = 10µm (A-D).